CR 86095
CR-86095

NAS12-554

INTERIM SCIENTIFIC REPORT

DEVELOPMENT OF ADVANCED DIGITAL TECHNIQUES FOR DATA ACQUISITION PROCESSING AND COMMUNICATION

By J. Levy and E.H. Gavenman

1 May 1968

Prepared under Contract NAS12-554(DO-C9)

National Aeronautics and Space Administration
Electronics Research Center
KC/Computer Research Laboratory
Cambridge, Massachusetts

Distribution of this report is provided in the interest of information exchange and should not be construed as endorsement by NASA of the material presented. Responsibility for the contents resides with the organization that prepared it.

ADVANCED COMMUNICATIONS INFORMATION MANAGEMENT

RESEARCH • DEVELOPMENT • ENGINEERING

ADCOM

A TELEDYNE COMPANY

Benjamin Goldstein and Robert M. Snow
Co-technical Monitors
NAS12-554
575 Technology Square
Cambridge, Massachusetts 02139

Requests for copies of this report should be referred to:

National Aeronatuics and Space Administration
Electronics Research Center
KC/Computer Research Laboratory
Cambridge, Massachusetts 02139

NAS12-554

INTERIM SCIENTIFIC REPORT FOR THE DEVELOPMENT OF ADVANCED DIGITAL TECHNIQUES FOR DATA ACQUISITION PROCESSING AND COMMUNICATION

By J. Levy and E. H. Gavenman

1 May 1968

Prepared under Contract No. NAS12-554(DO-C9) by

ADCOM
A Teledyne Company
808 Memorial Drive
Cambridge, Massachusetts

National Aeronautics and Space Administration
Electronics Research Center
KC/Computer Research Laboratory
Cambridge, Massachusetts

G-98

PRECEDING PAGE BLANK NOT FILMED.

TABLE OF CONTENTS

PRECEDING PAGE BLANK NOT FILMED.

LIST OF ILLUSTRATIONS

LIST OF TABLES

INTERIM SCIENTIFIC REPORT FOR THE
FOR THE DEVELOPMENT OF ADVANCED DIGITAL TECHNIQUES
FOR DATA ACQUISITION PROCESSING AND COMMUNICATION

By J. Levy and E.H. Gavenman

ADCOM, A Teledyne Company
Cambridge, Massachusetts

SUMMARY

This report reviews progress in the following study areas:

1. Characterization of Image Data Sources. Discussions of a design example of a Mars Television Mapping Mission, the effects of additive noise upon correct quantization of an analog voltage, the frequency response characteristics of vidicons, the statistical characteristics of video data, and the distorting effects of systematic errors upon data are presented.

2. Performance of Interpolation Algorithms. A performance comparison of zero order, first order and second order picture compression techniques, with simulated compressed picture material is contained herein.

3. Sensitivity of Compressed Picture Data to Channel Errors. The report includes a discussion and theoretical analysis of various error control techniques to be used with compressed picture data sent over a noisy link. Simulated reconstructed pictures illustrate the effectiveness of the line substitution approach.

PRECEDING PAGE BLANK NOT FILMED.

INTRODUCTION

General

This report covers work performed under Contract NAS12-554 (DOC9), Development of Advanced Digital Techniques for Data Acquisition Processing and Communication. The objectives pursued under this contract are:

> The characterization of image data sources, the development of new compression algorithms (second order and exponential interpolators), and evaluation of the sensitivity of compressed data to various error rates, and an evaluation of various error control techniques for reducing data sensitivity to errors.

Summary of Work During Reporting Period

a) The section entitled Design Example, Planetary Mapping Mission serves as a detailed study illustrating the methods for the selection of system parameters for a hypothetical large area television mapping mission of the planet Mars.

b) The probability of correct quantization of an analog voltage into one of m equal increment gray-levels depends upon both the number of gray-levels and the ratio of peak-to-peak analog signal-to-rms (Gaussian) noise level. An analytic treatment of this problem is found in the section entitled Analysis of Relationship Between Sensor Signal-to-Noise Ratio and the Number of Discernible Gray-Levels.

c) The section on Vidicon Frequency Response presents an analytic method for the evaluation of this important characteristic. Analytic results are found to display a functional form closely matching measured results for the RCA 7038 vidicon.

d) The section entitled Video Data Characteristics displays some approximate picture data autocorrelation functions as produced by digital computer evaluation of truncated segments of picture data. Brief discussions of other important data characteristics (correlation coefficients, spectral power density, relationship between aliasing error and sampling rate) are also to be found in this section.

e) Systematic errors introduced during the processing of data, as typified by offset, gain change and gain non-linearity serve to distort the data. The effects of these may be analytically stated in terms of various signal fidelity criteria (time-average error, root time-average square error, etc.); examples are evaluated for selected waveshapes.

f) The section entitled Summary of Performance of Compression Algorithms continues the analysis of second order compression algorithms and their comparison with zero order and first order algorithms. A determination of the bit compression ratios of the algorithms under study as a function of element compression ratio has been carried out (bit compression ratios are smaller than sample compression ratios on account of the necessary "overhead" of coding to specify significant sample locations). The description of a coding technique for the significant samples of a SOIOOT compressed picture is to be found in this section. Simulated compressed pictures, some of which first appeared in the previous Interim Report, and some of which are new with this report have been produced with the aid of a JPL plotter which yields pictorial material of an improved quality relative to those previously obtained.

g) A discussion and theoretical analysis of three interesting redundant error control techniques for the protection of compressed picture data transmitted over a noisy link is contained in the section entitled Study of Error Control Techniques for the Transmission of Compressed Pictures Over Noisy Binary Channels, and in Appendices A, B, and C. Theoretical performance comparisons of these schemes with the line substitution error control scheme described in the previous Interim Report are made. Simulations of the straight line substitution error control approach on ZOI and FOIOOT picutures at a bit error probability of 10^{-3} indicate a substantial improvement in reconstructed data quality relative to an uncontrolled picture. The most promising redundant error control scheme, which adds only three bits to each 11-bit ZOI sample word (or to each 12-bit FOIOOT sample word) should provide a slightly better quality picture than this in a 10^{-2} bit error probability environment.

ANALYSIS

Design Example, Planetary Mapping Mission

The conceptual design example selected for more detailed study in this report is a large area, television mapping mission of the planet Mars. This type of mission could be applicable to Voyager class exploration from the orbiting vehicle. Since the design example is for purposes of illustration only assumed mission parameters are presented without justifying arguments. The assumed orbit and vehicle parameters are as follows.

Orbit size:	1800 × 36,000 km
Obit period:	~ 25 hours
Velocity at periapsis:	3700 m/sec
Sub-satellite track shift/orbit:	5.85 degrees
Required surface coverage:	170 × 170 km
Camera field-of-view at periapsis:	5.35 degrees
Vehicle stabilization:	$\pm 1^{\circ}$ on all axes, 2000 second limit cycle
Angular camera motion:	3.5×10^{-5} rad/sec

Sensor requirements assumed and/or determined from the preceding assumptions include the following.

Resolution:	100 meters at periapsis
Optical field-of-view:	7.35 degrees
Motion smearing:	<50 meters (equivalent to 90% response at 100 meter resolution)
Sensor image format:	1" × 1"
Number of resolution elements per TV scan line using Kell factor of 0.7:	2500
Optical resolution: (Blur spot diameter at edge of image)	$< 4 \times 10^{-4}$ inches
Time between exposures:	> 46 seconds
Exposure time: (for 50 meter smearing)	13.5 milliseconds

A Schmidt lens system yields the smallest size angular blur spot off axis, for a given f number, of all conventional lens systems. The off axis angular blur spot of a Schmidt lens system is given by

$$\beta = .0417\, \theta^{2}\, \nu^{-3} \qquad (1)$$

where

β = angular blur spot (radians);

θ = angle off axis; and

ν "f number" describing aperture.

Assuming a relative aperture of f/4 ($\nu = 4$) and a focal length of four inches ($\theta_{max} = 7.1^{o}$), the maximum angular blur spot is about 10^{-5} radians. Thus the optical resolution of the system is about 25,000 lines per inch, ten times greater than required for the overall system. The effective aperture of this lens system would be one inch.

To specify other design parameters of the sensor system it is necessary to establish scene illumination characteristics. The surface brightness of Mars, at local noon, may be determined from:

$$F_{E} = \frac{E_{o}\rho_{a}}{\pi d^{2}} \qquad (2)$$

where

F_E = scene brightness in foot-lamberts;

E_o = luminous solar constant = 1.25×10^{4} foot candles;

d = mean solar distance = 1.524 astronomical units; and

ρ_a = local albedo; ρ_a is estimated to vary between 0.05 and 0.3.

The scene brightness at noon varies from 86 to 515 foot-lamberts with the average estimated to be about 258 foot-lamberts. Scene brightness will decrease as the solar incidence angle θ increases ($\theta = 0$ at noon); the decrease is approximately equal to cos θ. If photos are also desired near the terminator (e.g., $\theta = 84^{o}$), the scene brightness might vary from a minimum of about 10 foot-lamberts to a maximum of about 515 foot-lamberts. Thus the sensor dynamic range must be at least 50:1. Most space television systems use devices with dynamic ranges of at least 100 : 1.

The desired system resolution of 2500 elements per scan line, may be achieved through the use of a 2 inch return beam vidicon. Such a tube was developed for the EROS program for which the maximum exposure level was specified as 0.01 foot-candle-seconds. The faceplate illumination level is related to scene brightness by:

$$F_S = \frac{F_E T}{4 \nu^2} \qquad (3)$$

where

F_S = faceplate illumination in foot candles;

T = lens transmission (assume 0.5 as reasonable value); and

ν = lens f number = 4.

The maximum illumination is therefore about 4.0 foot candles. Assuming an additional illumination loss factor of 0.5 due to the vidicon photo conductor, the effective illumination level is about 2.0 foot candles. Therefore the maximum exposure time per frame is 5.0 milliseconds based on a maximum exposure level of 0.01 foot-candle-seconds.

Smearing caused by vehicle motion during the exposure period is determined by:

$$S = (\omega r + v)\Delta t \qquad (4)$$

where

ω = angular velocity of the camera due to limit cycling = 3.5×10^{-5} rad/sec;

r = vehicle altitude = 8,000 km maximum;

v = vehicle velocity at periapsis = 3.7 km/sec; and

Δt = exposure time = 5.0 milliseconds.

Therefore the maximum smearing should be on the order of 20 meters, well within desired system objectives.

Measurements of return beam vidicon performance indicate a peak-to-peak signal-to-rms noise ratio of 10:1 (20 dB) is obtained at an exposure level of 7.6×10^{-4} foot-candle-seconds. Therefore a peak exposure level of 10^{-2} foot-candle-seconds is indicative of a signal-to-noise ratio of about 130:1 (42 dB). It is important to note that signal-to-noise ratios are also affected by read out rate. The quoted signal-to-noise ratios are based on an elemental scan (or read out) time of about 200 nanoseconds. Thus the equivalent line scan time is 500 microseconds yielding a complete frame read out time of 1.25 seconds (500 μsec/line $\times$ 2500 lines).

The vidicon output signal would be stored on an analog tape recorder. The tape output could then be digitized to produce the desired PCM data stream for transmission.

Analysis of Relationship Between Sensor Signal-to-Noise Ratio and the Number of Discernible Gray Levels

The gray-scale capability of a video system depends upon the linearity of its transfer function (intensity "in" vs. intensity "out"), its dynamic range, and its output signal-to-noise ratio (SNR). Assuming that the transfer function is linear and has sufficient dynamic range, the number of different gray levels between black and white that can be detected with a given confidence is determined by the output noise level and the sensitivity of the viewing device. If the viewing device (e.g., the human eye or a photometer) is capable of discerning video signal changes smaller than the effective noise level, the noise alone is the limiting factor. For the following discussion it will be assumed that noise is the limiting factor.

If the output display is being interpreted on a "large-area" basis, that is, where the gray levels of portions (areas) of the display containing many resolution or "picture" elements are of importance, small errors in the individual elements can be tolerated without noticeable degradation to picture quality. In this case it is reasonable to assume that the discernable gray-level change is limited by the rms noise level. However, if the gray-level of each individual picture element is of importance (e.g., if the display is being analyzed with a microphotometer), then the accuracy to which the gray-levels should be interpreted is limited by peak noise levels.

The analysis below evaluates the probability of correct quantization of an analog voltage into one of m equal increment gray-levels in the presence of an additive Gaussian noise perturbation.

The size of each increment is equal to ΔA volts where

$$\Delta A = \frac{A}{m-1}. \qquad (5)$$

Any voltage lying within $\pm \frac{\Delta A}{2}$ of the i^{th} gray-level will be encoded as A_i volts, as illustrated in Fig. (1a).

Attention is focused upon the i^{th} gray scale zone, which the analog signal voltage is considered to occupy. It is assumed that the signal is equally likely to be at any amplitude within this quantization increment. The probability density function of this signal is illustrated in Fig. (1b); the probability density function of the noise is shown in Fig. (1c).

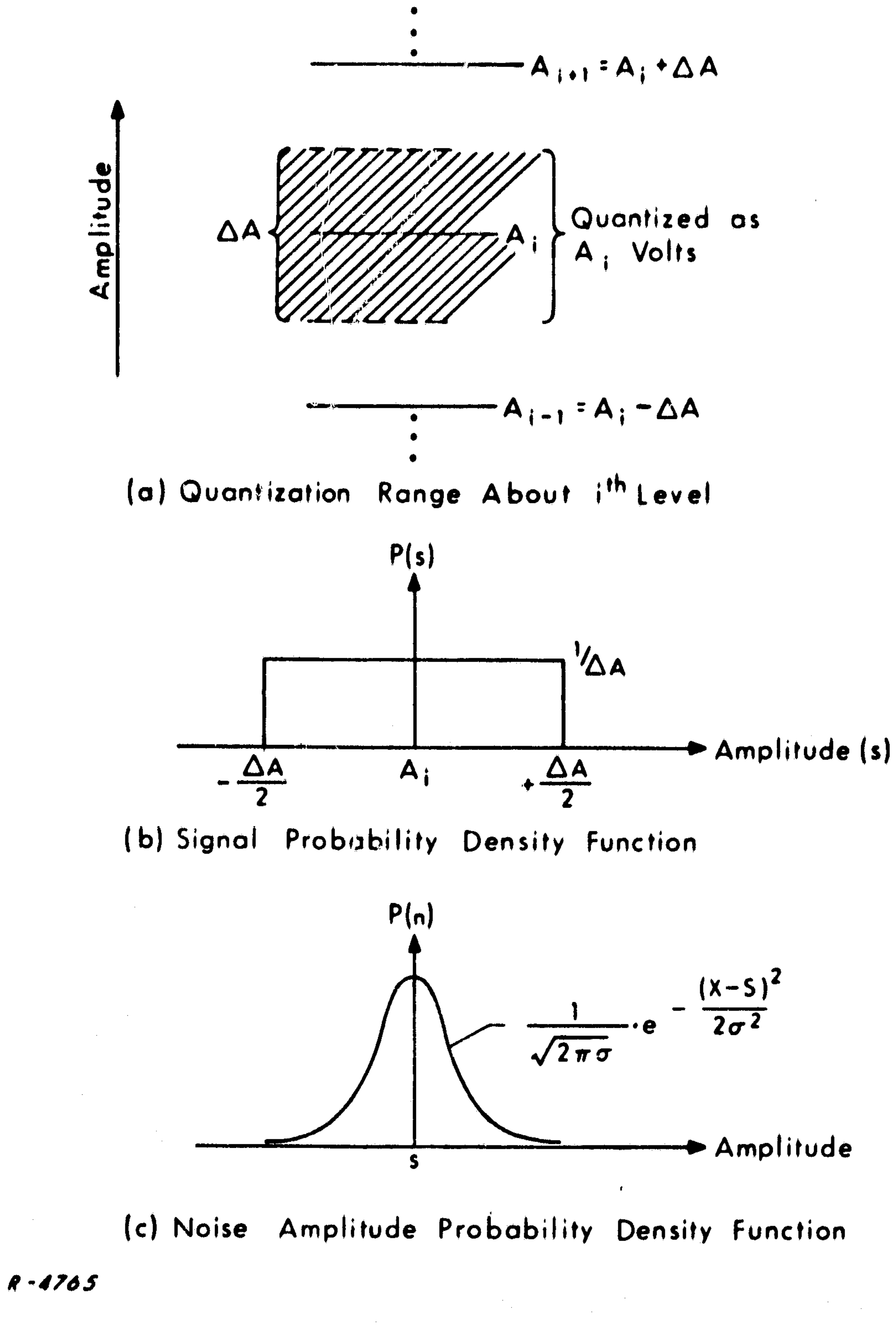

Figure 1 Signal and Noise Probability Density Functions in the Vicinity of i^{th} Quantization Level

The probability of correctly quantizing a particular signal sample, given that its noiseless value lies within the i^{th} cell is easily obtained. First note that when the signal-related voltage $S - A_i$ has the particular value y, the probability of correct quantization is:

$$P_c(y) = \int_{\frac{-\Delta A}{2} - y}^{\frac{\Delta A}{2} - y} \frac{1}{\sqrt{2\pi}\,\sigma} e^{-x^2/2\sigma^2} dx \qquad \frac{-\Delta A}{2} \leq y \leq \frac{+\Delta A}{2} \tag{6}$$

or, in terms of a normalization of Eq. (6) above to place a Gaussian density with unit standard deviation inside the integrand:

$$P_c(\hat{y}) = \int_{\frac{-\Delta A}{2\sigma} - \frac{\hat{y}}{\sigma}}^{\frac{\Delta A}{2\sigma} - \frac{y}{\sigma}} \frac{1}{\sqrt{2\pi}} e^{-x^2/2} dx \qquad \frac{-\Delta A}{2\sigma} \leq \hat{y} \leq \frac{+\Delta A}{2\sigma} \tag{7}$$

The function $P_c(y)$ for $\frac{-\Delta A}{2} \leq y \leq \frac{+\Delta A}{2}$ is plotted in Fig. 2 for various ratios of $\Delta A/2\sigma$. The construction was made using tables of the normal probability integral. The probability of correct quantization is obtainable by the integration of $P_c(\hat{y})$ across the uniformly distributed signal voltage variable:

$$P_c = \frac{\sigma}{\Delta A} \int_{\frac{-\Delta A}{2\sigma}}^{\frac{+\Delta A}{2\sigma}} P_c(\hat{y})\, d\hat{y} \tag{8}$$

The indicated integration may readily be performed from Fig. 2 by graphical means providing the following results:

$\frac{\Delta A}{2\sigma}$	P_c
1	.61
2	.78
3	.87
4	.90

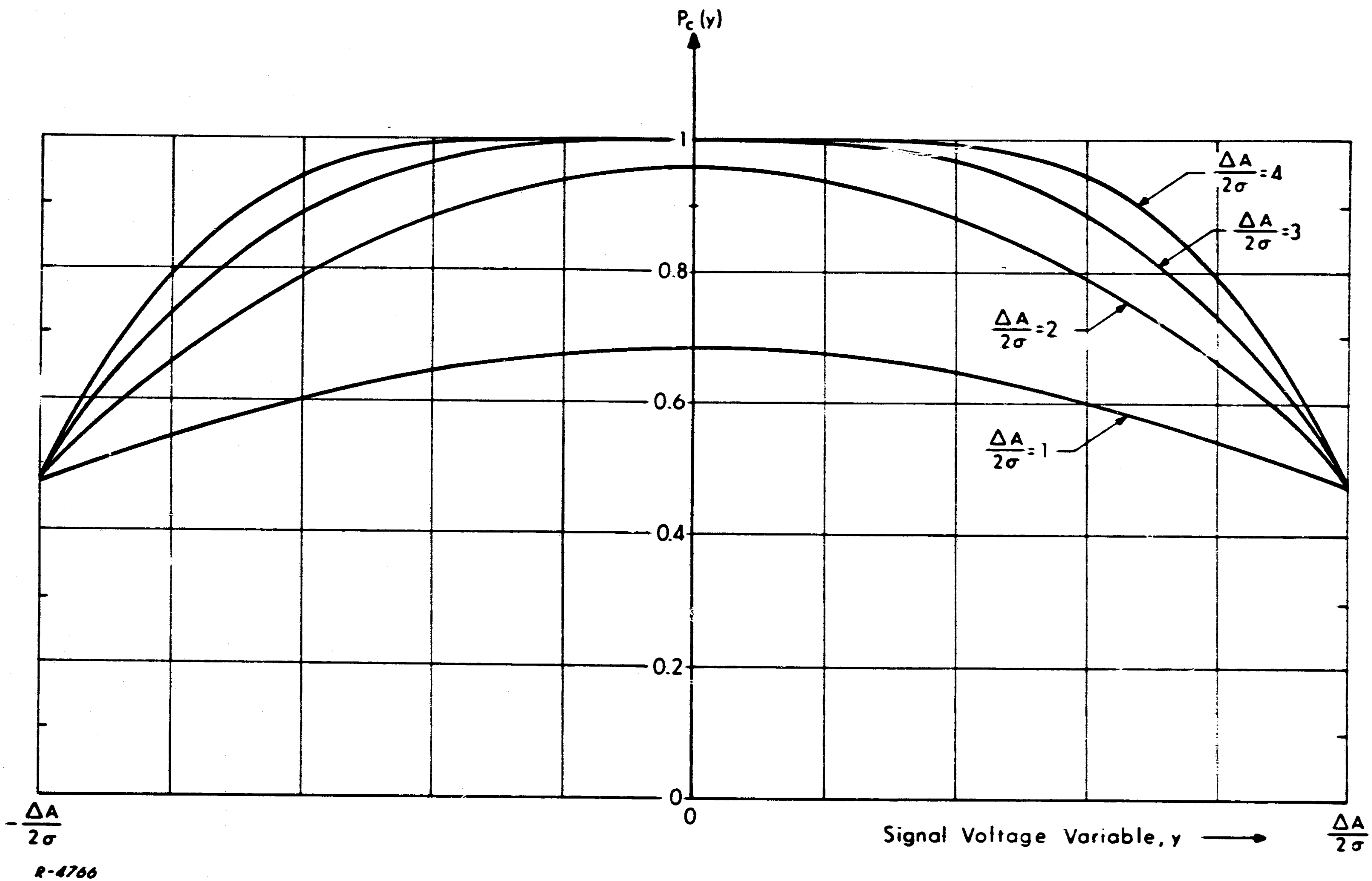

Figure 2 $P_c(y)$ as a Function of $\Delta A/2\sigma$

The quantization cell width, ΔA, was defined earlier to be $A/m-1$. Therefore, $\Delta A/2\sigma$ ratios of 1, 2, 3 and 4 define peak-to-peak signal to rms noise ratios of 2(m-1), 4(m-1), 6(m-1) and 8(m-1) respectively. Figure 3 illustrates the relationship between signal-to-noise ratio, the number of gray-levels to be quantized and the probability that the vidicon signal will be correctly quantized.

As was noted previously in the section entitled Design Example, Planetary Mapping Mission, the ratio of peak-to-peak signal to rms noise with a 0.01 foot-candle-second exposure should be 130 : 1 (42 dB). Because of the very high gain in the multiplier section of this tube, noise figures in later amplification stages will not degrade this SNR. Referring to Fig. 3 it can be seen that this SNR is likely to be adequate only for "large-area" interpretation when the signal is quantized to 64 levels (6 bits), since almost 39 percent of all picture elements will be quantized incorrectly.

For microphotometric analysis the number of meaningful gray-levels probably lies between 16 and 32 for this example case based on the results shown in Fig. 3.

Vidicon Frequency Response

The limiting factor which determines the frequency response characteristics of a vidicon is the scan beam size and energy distribution shape. It has been shown experimentally that beam (energy distribution) shape is approximately Gaussian and due to its finite size if it scans a scene which has a resolution finer than the beam spot, there will be a significant loss in the transmitted resolution. The conventional methods of describing vidicon frequency response characteristics is to draw a curve of square-wave amplitude response versus TV line number. The term "TV line number" is used here to describe the number of half-cycles of square wave test pattern per scan line. (A full cycle is a consecutive black-white pair). On the basis of an assumed "square" picture having equal picture resolution in both horizontal and vertical directions, the TV line number is in fact equal to the number of lines in the picture. Frame rate and TV line number serve to determine the characteristic video signal bandwidth (See Eq. (19) below).

A physical description of vidicon operation is as follows. Suppose that the tube face is exposed to an optical square wave pattern. Inside the tube there is a thin photoconductive surface, each element of which is an insulator in the dark but becomes slightly conductive when it is illuminated. When the pattern is focused on the photoconductor surface, each illuminated element conducts slightly in accordance with the level of illumination on the element. This causes the potential of its opposite surface (on the gun side) to rise. Hence, there appears on the gun side of the entire surface

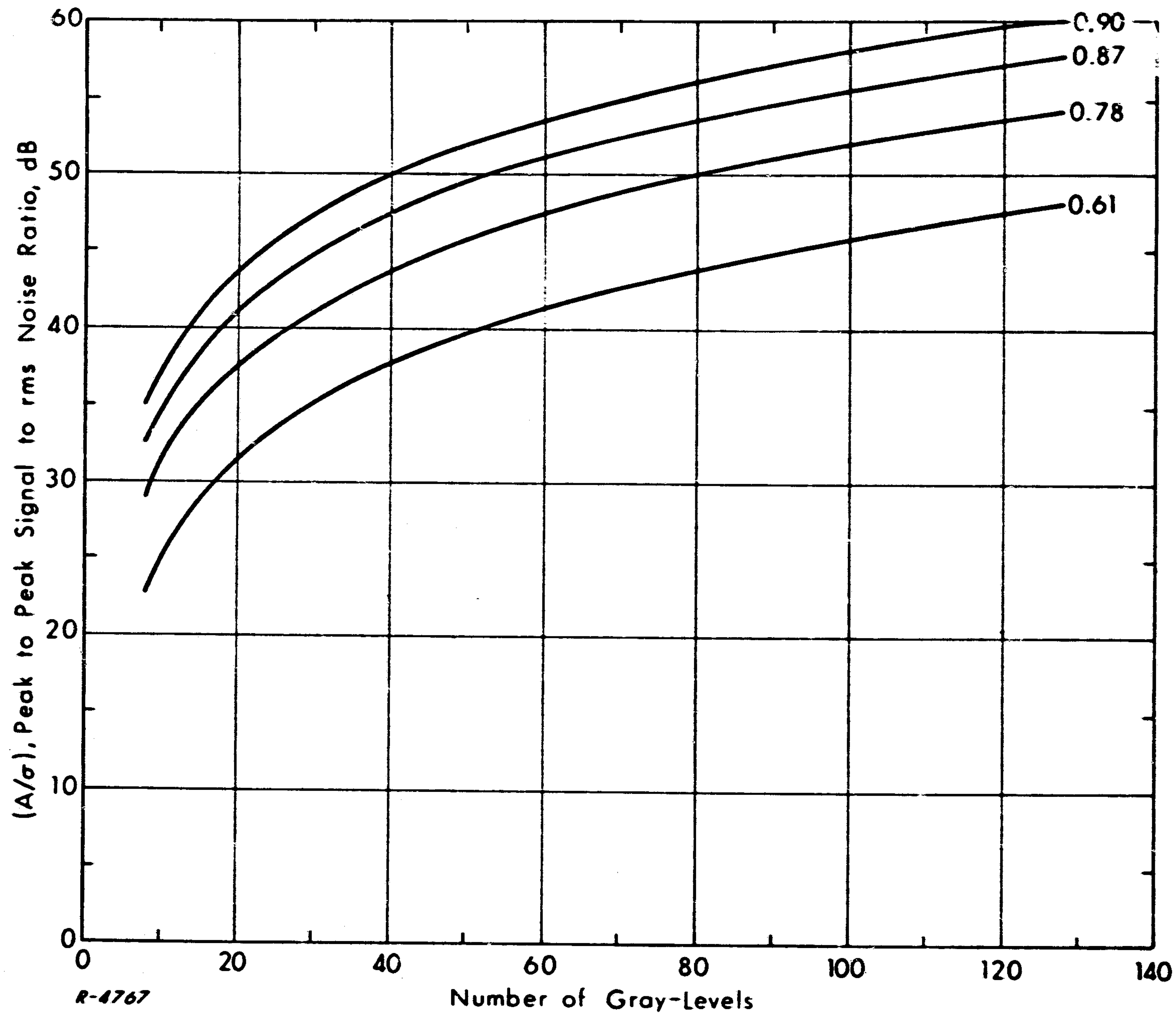

Figure 3 Relationship Between Number of Gray-Scale Levels and Signal-to-Noise Ratio for Various Probabilities of Correct Quantization

an alternating, positive potential pattern corresponding to the pattern of light intensity focused on the tube.

When the gun side of the photoconductive surface is scanned by the electron beam electrons are deposited from the beam thereby reducing the elemental potential differences across the photoconductor. When the two surfaces of the photoconductive surface, which in effect is a charged capacitor, are connected through the external target (signal-electrode) circuit and the scanning beam, a capacitive current is produced which constitutes the video signal. The magnitude of the current is proportional to the surface potential of each element being scanned and t rate of scan.

In effect, if the illumination pattern consists of the alternate black and white bars of a square wave pattern, the photoconductive surface can be visualized as a mosaic of small photoconductors with equal size apertures separated by spaces of equal dimensions. If one of these photoconductors were scanned by an infinitesimally narrow electron beam its response would be as follows.

$$f(t) = A, \quad -\delta/2 \leq t \leq \delta/2 \tag{9}$$

where

δ = aperture size (scan time) in seconds

However the electron beam has nonzero width and its energy distribution shape is approximately Gaussian. Thus the photoconductor can be represented in terms of an impulse response. This describes the photoconductor response time function as it sweeps past a high intensity infinitesimally narrow light speck on the surface.

$$h_o(t) = \frac{B}{\sqrt{2\pi}\,\sigma} e^{-\frac{1}{2}(t/\sigma)^2} \tag{10}$$

where σ is the standard deviation describing the spread of the beam.

The description given by Eq. (10) assigns an impulse response to the beam which is equivalent to the impulse response characterization of a linear filter. The beam response is the analog of an unrealizable electric filter, since $h_o(t)$ has nonzero values for $t < 0$.

If the beam sweeps across an isolated light intensity pulse as in Eq. (9) then the total video signal produced at any instant is due to the contributions of infinitesimal intensity elements on the scanned surface all weighted by $h_o(t)$ in accordance with Eq. (10), t being the (time) displacement between the infinitesimal element and the center of the scanning beam. In fact this weighted infinite summation is nothing more than the convolution integral so frequently used to evaluate the response of an electrical network to an input function:

$$g(t) = \int_{-\infty}^{+\infty} h_o(\tau)\, f(t-\tau)\, d\tau \tag{11}$$

The substitution of Eq. (9) and (10) into Eq. (11) leads to evaluation of the video signal produced in response to an isolated pulse of constant intensity:

$$g(t) = 1 - \Phi\left(\frac{\delta}{2\sigma} - \frac{t}{\sigma}\right) - \Phi\left(\frac{\delta}{2\sigma} + \frac{t}{\sigma}\right) \tag{12}$$

where

$$\Phi(x) \equiv \int_{x}^{\infty} \frac{1}{\sqrt{2\pi}}\, e^{-y^2/2}\, dy \tag{13}$$

and g(t) has been normalized to have a maximum value of unity.

The response signal is strongly dependent on δ/σ, the ratio of the width of the pulse to the width of the beam. Figure 4 illustrates the response g(t) for the three cases: $\delta/\sigma >> 1$, $\delta/\sigma = 4$, and $\delta/\sigma = 2$. Note that as the beam grows in thickness the distortion and spreading of the video pulse increases. The pulses shown in Fig. 4 only indicate the response of a single element aperture. When δ/σ ratios are less than four, crosstalk between adjacent pulses (or apertures) of the square wave pattern further reduces the peak-to-peak amplitude excursions of the pulse train. For example, when $\delta/\sigma = 2$ the peak response of a single pulse will be reduced to about 0.68 of its value for $\delta/\sigma >> 1$. In addition, its amplitude at time $t = \delta$ (half the interval between successive peaks) has only fallen to 0.16 of its peak ($\delta/\sigma >> 1$) value. At this time the rising edge of the following pulse will have reached the same value resulting in a combined amplitude of 0.32. Thus the peak-to-peak excursion of the pulse train will be only 0.36 of its optimum value for an infinitesimally narrow beam.

The frequency characteristics of the output signal pulse train in response to the square wave pattern can be determined by multiplication of the Fourier series coefficients of the square wave with the transform

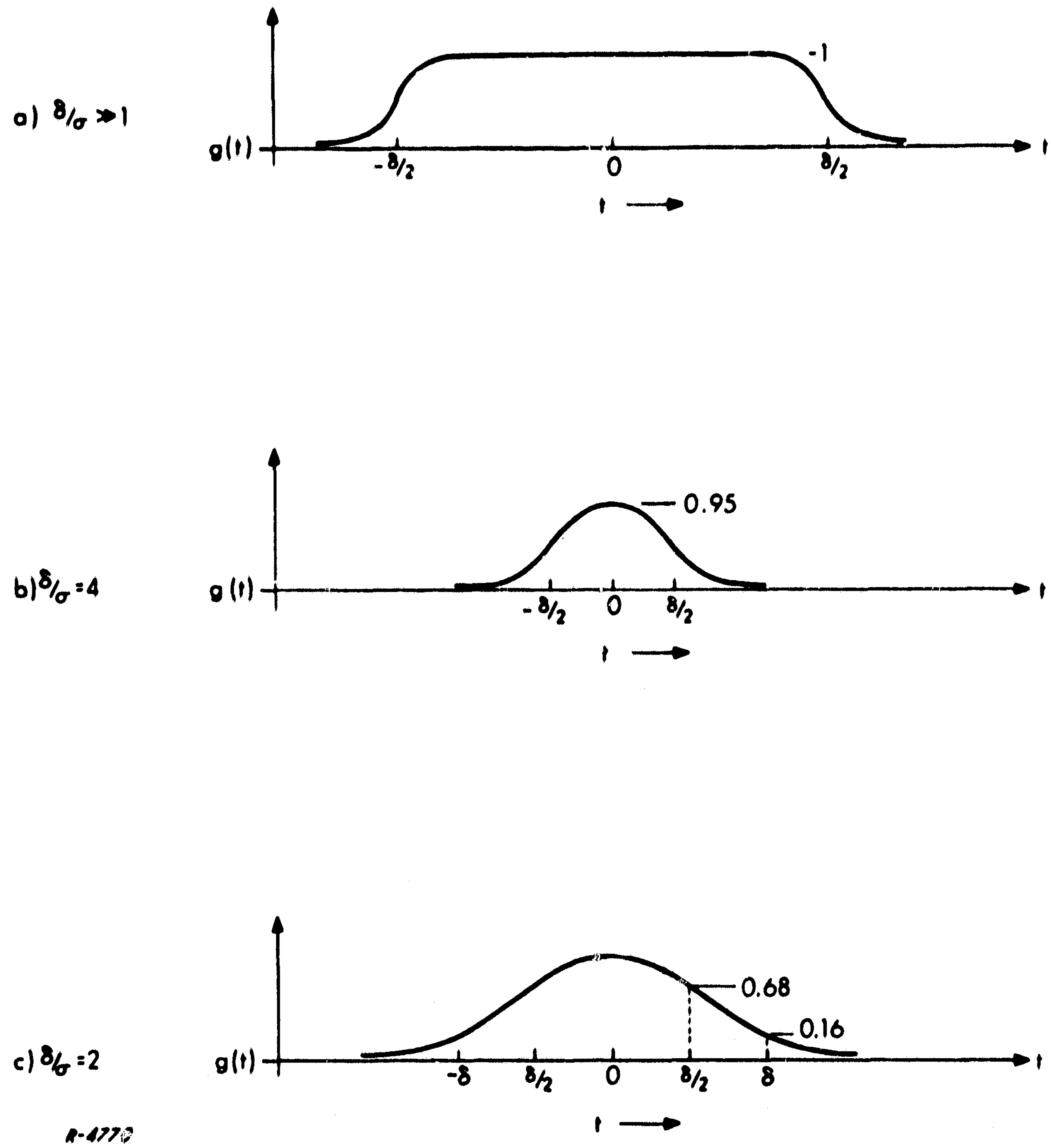

Figure 4 Typical Vidicon Response to a Rectangular Pulse Test Pattern as Functions of Scan Time to Beamwidth Ratios

of the Gaussian beam function. The latter is given by the Fourier integral:

$$H_o(\omega) = \frac{B}{\sqrt{2\pi}\,\sigma} \int_{-\infty}^{\infty} e^{-\frac{1}{2}(t/\sigma)^2} e^{-j\omega t} dt \qquad (14)$$

The transform function also has a Gaussian shape:

$$H_o(\omega) = Be^{-\frac{1}{2}(\sigma\omega)^2} \qquad (15)$$

The spectrum of a square wave train repeating its cycle every T seconds, and assumed to continue indefinitely for all time is a pure line spectrum. It is thus representable as the sum of a series of impulses located at discrete frequencies and with impulse areas (i. e., component amplitudes) weighted by the characteristic sin x/x spectral function associated with a square pulse. The spectrum is:

$$F(\omega) = A \cdot \sum_{\substack{n=0,\text{ and}\\ \text{all odd integers}}} \left[\frac{\sin(n\pi/2)}{(n\pi/2)}\right] u\left(\omega - \frac{2\pi n}{T}\right) \qquad (16)$$

where u( ) denotes the unit impulse function.

There are lines present at dc, and at all the frequencies 1/T, 3/T, 5/T,... Hz.

The total vidicon output spectrum in response to the square wave test pattern may therefore be represented as follows,

$$G(\omega) = AB \cdot \sum_{\substack{n=0,\text{ and}\\ \text{all odd integers}}} \left[\frac{\sin(n\pi/2)}{(n\pi/2)}\right] \cdot e^{-\frac{1}{2}\left(\frac{2n\pi\sigma}{T}\right)^2} u\left(\omega - \frac{2n\pi}{T}\right) \qquad (17)$$

Equation (17) states the square wave response in rather general form. The output consists of the square wave spectrum with attenuation of the higher harmonics, i. e., a distorted square wave. A good approximation to the level of response of a vidicon to a square wave pattern of a given "frequency" is best obtained by calculating the relative level of the exponential term in Eq. (17) at the fundamental frequency ($1/T = 1/2\delta$) of the square wave:

$$R(\omega) = e^{-\frac{1}{2}\left[\frac{\pi\sigma}{\delta}\right]^2} \qquad (18)$$

Figure 5 compares an experimental curve of the RCA type 7038 vidicon with one calculated from Eq. (18) above. Standard video scan rates (one line swept out every 63.5 μsec) have been assumed. The "calculated" curve represents a selection of σ = 81.4 nanoseconds, which was found by trial and error to provide a close match to the measured curve. The close fit of the two curves serves to validate our analytic description of vidicon response. Video bandwidth in Fig. 5 is given by the following relationship:

$$f = \frac{1.6 \times \text{number of elements/line}}{2 \times 63.5 \times 10^{-6} \text{ seconds/line}} = \frac{1.6}{2\delta} \text{ Hz} \qquad (19)$$

The preceding discussion is also applicable to the return beam vidicon tube. However the return beam vidicon uses a specially designed focus and deflection coil system which reduces the scan beamwidth (σ) by a factor of about 2.5. The computed return beam vidicon frequency response of Fig. 6 is applicable to a system with parameters the same as those evolved in the section entitled "Design Example, Planetary Mapping Mission": a line scan period of 500 microseconds and a frame time of 1.25 seconds. The significance of this curve is that it allows the system designer to specify accurately the required response of an image enhancement filter to compensate for roll-off in the vidicon response. The compensation procedure for the system is illustrated in Fig. 7. To avoid overemphasis of high frequency noise, the maximum frequency to be accurately compensated is arbitrarily selected to be 14.4 MHz; this is the point at which the vidicon amplitude response has decreased to a value of 0.2.

Because of the high bandwidth capability of the return beam vidicon, external data handling devices (e.g., a tape recorder) would limit the frequency response capability of the imaging system for many space applications to about 4 MHz. From Fig. 6 it can be seen that for such applications little or no vidicon compensation would be required in the hypothetical system.

Video Data Characteristics

The preceding section has discussed the frequency response characteristics of the vidicon imaging tube. The question of the actual frequency characteristics of video data next arises. This study has found an absence of useful reference material on this subject. Furthermore, the computer costs required to perform investigation of a basic picture data parameter such as power spectral density are prohibitive. Therefore the following discussion of limited scope has been prepared.

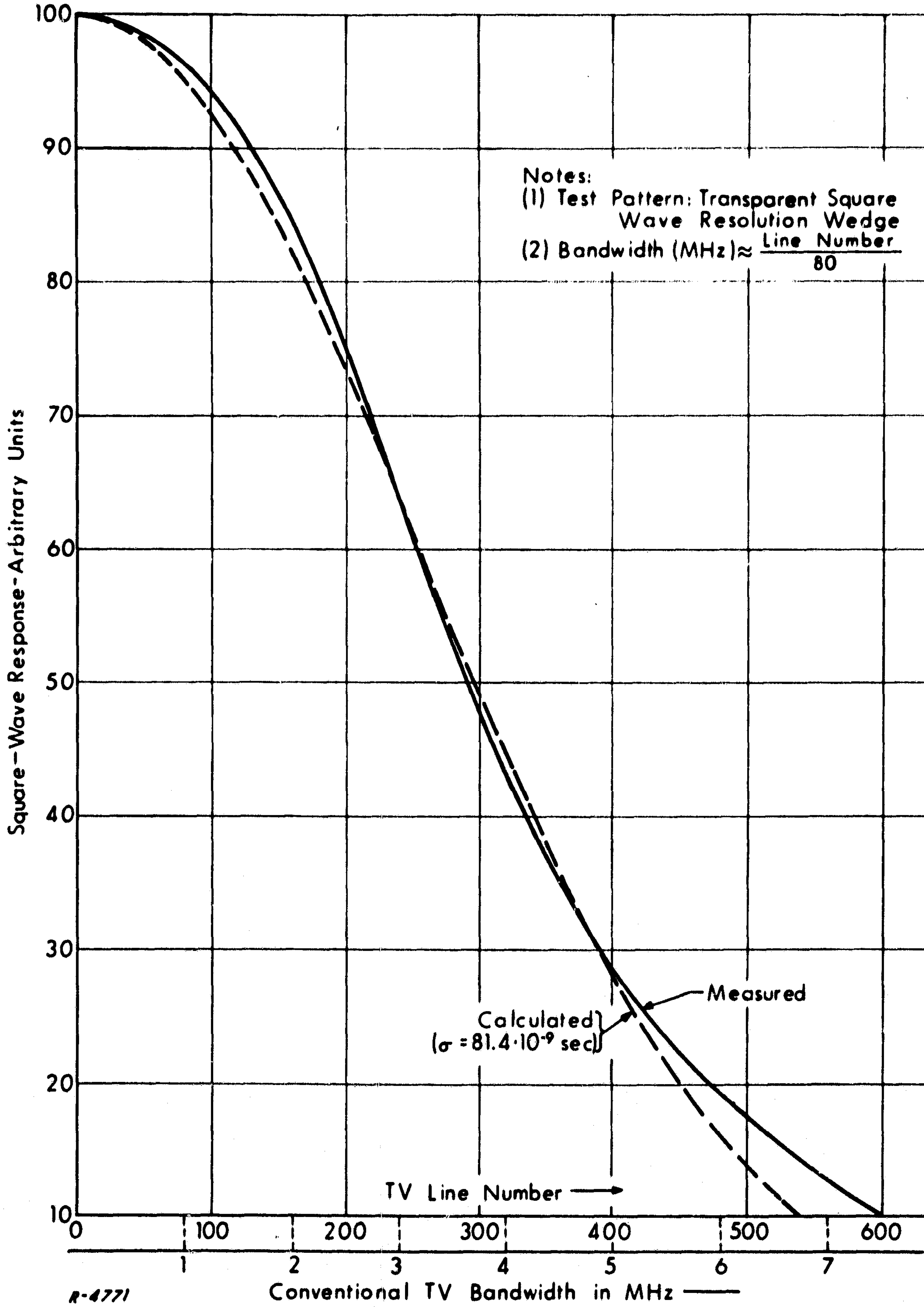

Figure 5 Uncompensated Horizontal Square-Wave Response of RCA Type 7038 Vidicon

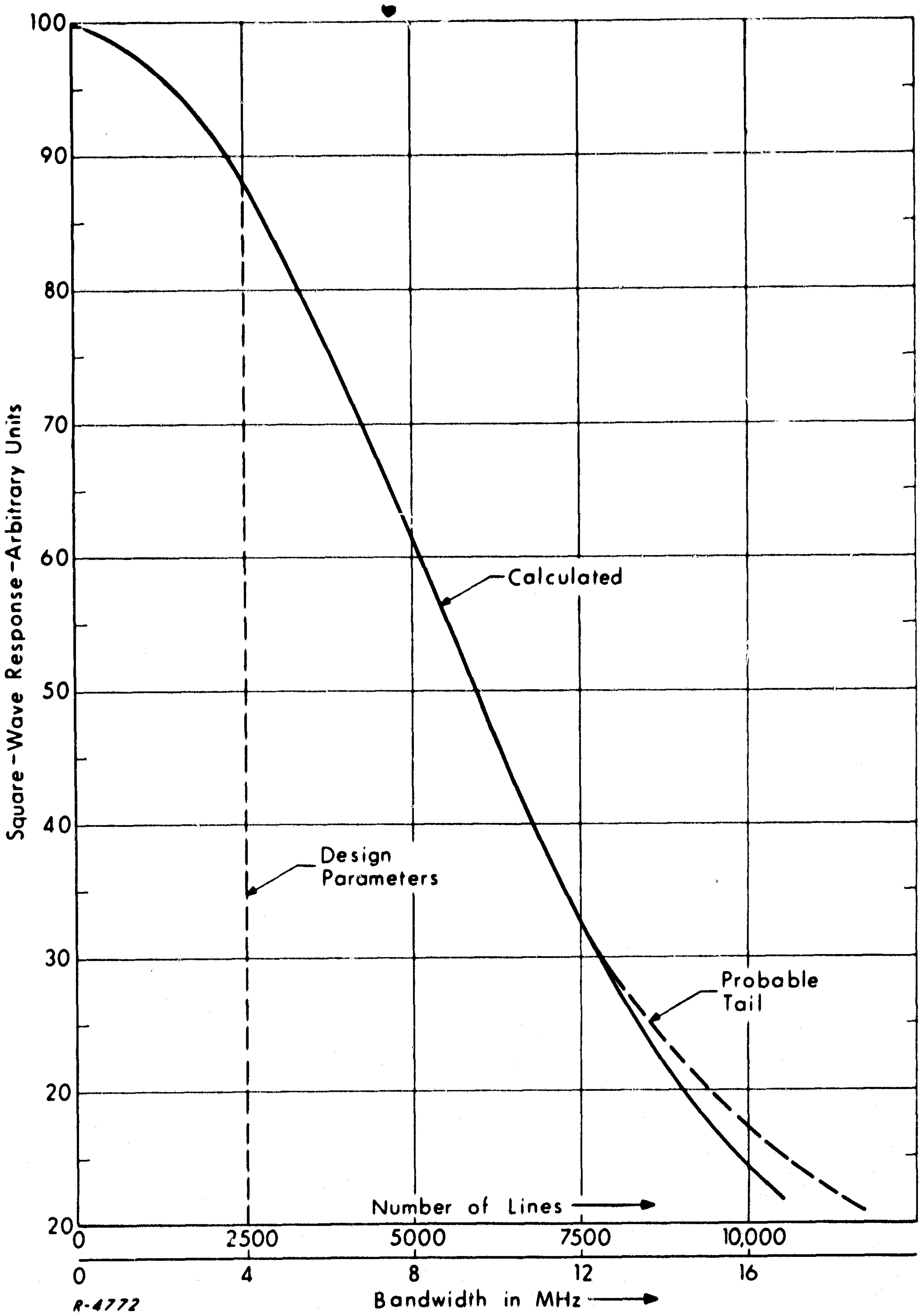

Figure 6 Return Beam Vidicon Frequency Response— Hypothetical System Scan Rates Identical to those For Mars TV Mapping Mission Example

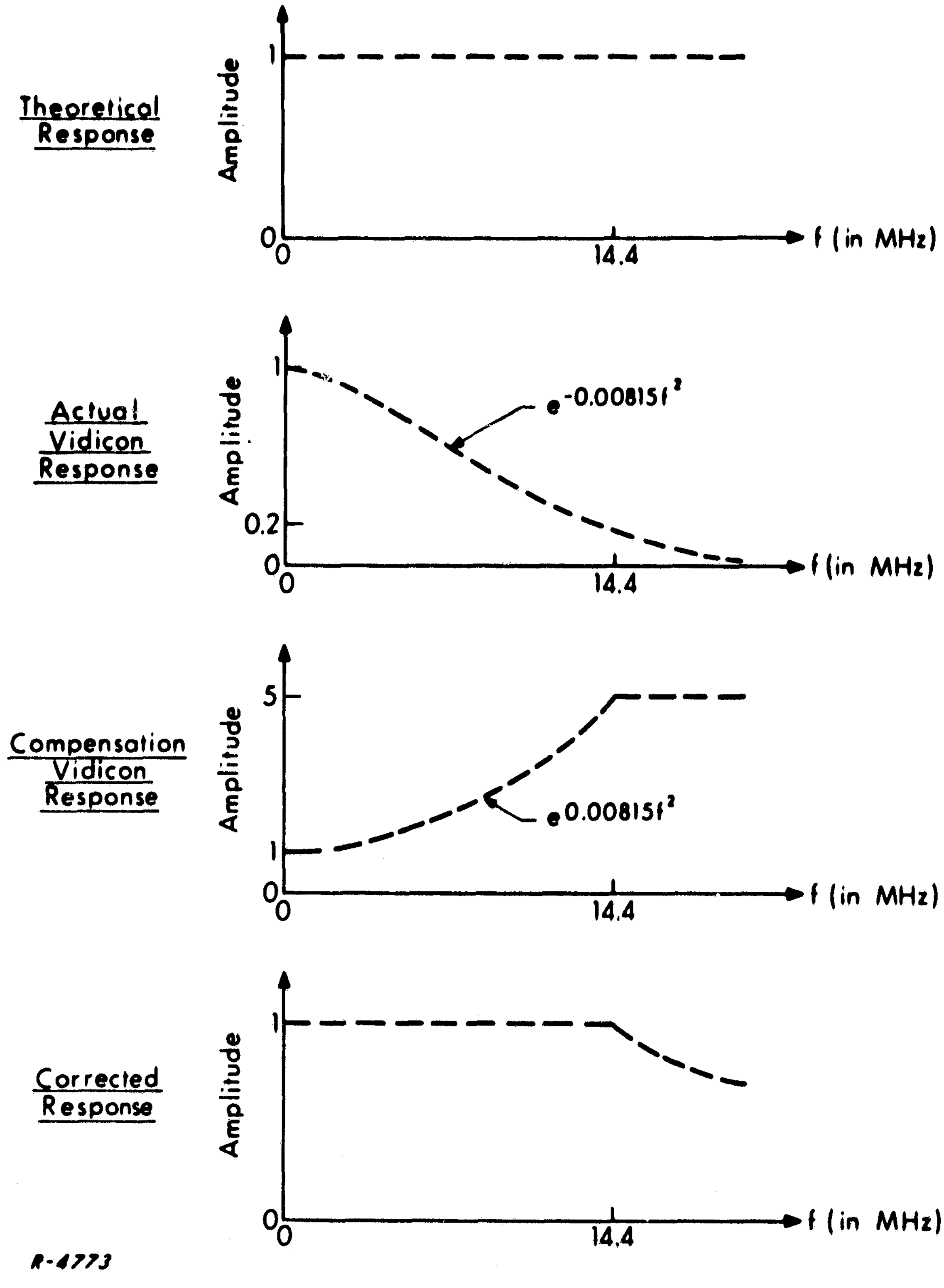

Figure 7 Vidicon Frequency Response Compensation For Mars TV Mapping System Example

The power spectral density and the autocorrelation function of a waveform represent a Fourier transform pair. Calculation of the autocorrelation function is simple though very time consuming. However some insight can be gained by inspection of a truncated autocorrelation function utilizing only three scan lines of data.

The available data consists of a sequence of samples from the continuous video data waveform process. The sampled data from the truncated picture segment is a sequence of data values $x_1, x_2, \ldots x_m$, each of which has as its sample value one of the integers from 0 to 63 inclusive. These samples are equally spaced in time by some sampling interval Δ and hence the simulation enables us to evaluate the autocorrelation function for values of time separation which are multiples of this interval, from which the continuous curve may easily be produced.

Stationarity of the data is assumed to exist over the truncated interval. This permits us to refer to an ordinary autocorrelation function $R(\tau)$:

$$R(\tau) \equiv E\{x(t) \cdot x(t+\tau)\} \tag{20}$$

In terms of the m samples in the truncated data set, it is possible to evaluate $R(\tau)$ by computation for shifts of an integer number of sample intervals:

$$R(n\Delta) \cong \sum_{i=1}^{m-n} x_i \cdot x_{i+n} \tag{21}$$

The autocorrelation function may be normalized so that its maximum value (which always occurs at $\tau = 0$ and is equal to the mean squared value of the variable x) is unity:

$$\Phi(\tau) = \frac{R(\tau)}{\overline{x^2}} = \frac{R(\tau)}{\sigma^2 + \mu^2} \tag{22}$$

where σ and μ are the respective standard deviation and mean of x.

$\Phi(\tau)$ was computed in this manner in four different areas of a high resolution photograph. For these examples, τ was allowed to vary from zero to 450 elements, the number of elements in a scan line. The results of these computations are presented as Fig. 8. The following features of $\Phi(\tau)$ should be noted:

1. The function is non-negative and has a high mean value.

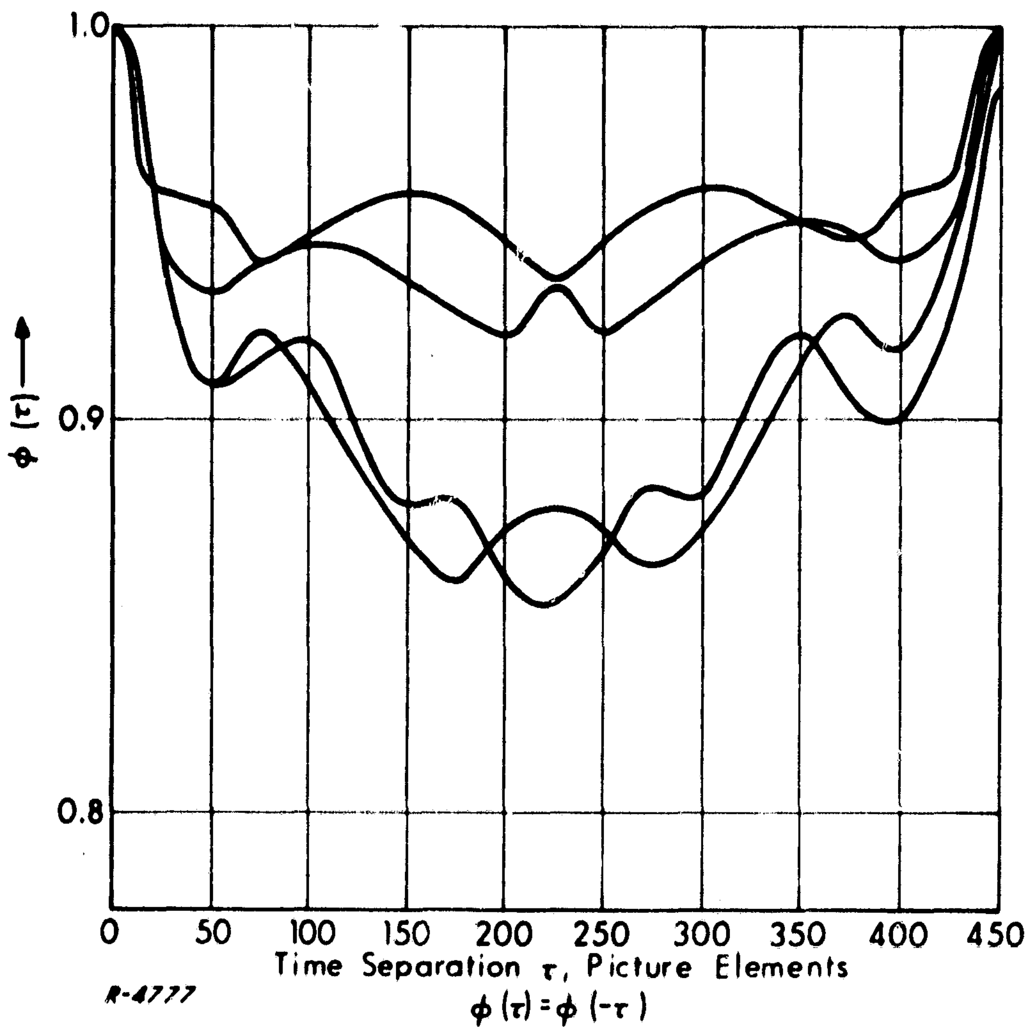

Figure 8 Normalized Autocorrelation Function Examples (High Resolution Reconnaissance Photo)

2. Peaks in the function occur at time shifts equal to the length of a scan line. This high line-to-line correlation should be expected since image content would normally be independent of the direction of scan. Correlation peaks should also be expected at multiples of the scan line length; however these peaks should decrease rapidly in magnitude.

3. Minimum correlation occurs when τ is approximately equal to half the scan line length. This is to be expected since points so widely separated in space have little in common with respect to image-describing information content.

Figure 9 is a representation of what might be expected for a full frame normalized autocorrelation function. The long, flat "tail" for large separations is indicative of completely uncorrelated data; the non-zero value is due to the nonzero mean value of the data, as is discussed in more detail below.

The power spectrum of the data will be the transform of $\Phi(\tau)$. Little can be said concerning its characteristics except that the dc power content will be significant and the damped periodic structure of the autocorrelation function will produce some power peaking at the line scan frequency (2 kHz in the Mars mission example).

If significant power is found at frequencies in excess of the maximum satisfying the Nyquist criterion (e.g., above $2.5 \cdot 10^6$ Hz for the $5 \cdot 10^6$/sec sampling rate needed for the Mars mission system), past vidicon filtering is required to minimize "aliasing" errors. The Mars mission system example would require such filtering because the optical resolution is greater (25,000 elements per scan line) than required. Since the vidicon can respond to frequencies of at least 16 MHz (10,000 elements per scan line), large quantities of power may exist above 2.5 MHz. This high frequency power is not required to meet the resolution requirements of the system (2500 elements per scan line) and hence can be filtered. It appears that a well-designed system should utilize optics with a resolution just equal to the system requirements.

It is most important to stress that $\Phi(\tau)$ is a valuable descriptor of data characteristics, but it does not present data correlations on a meaningful scale if the data variable has a nonzero mean value. A proper

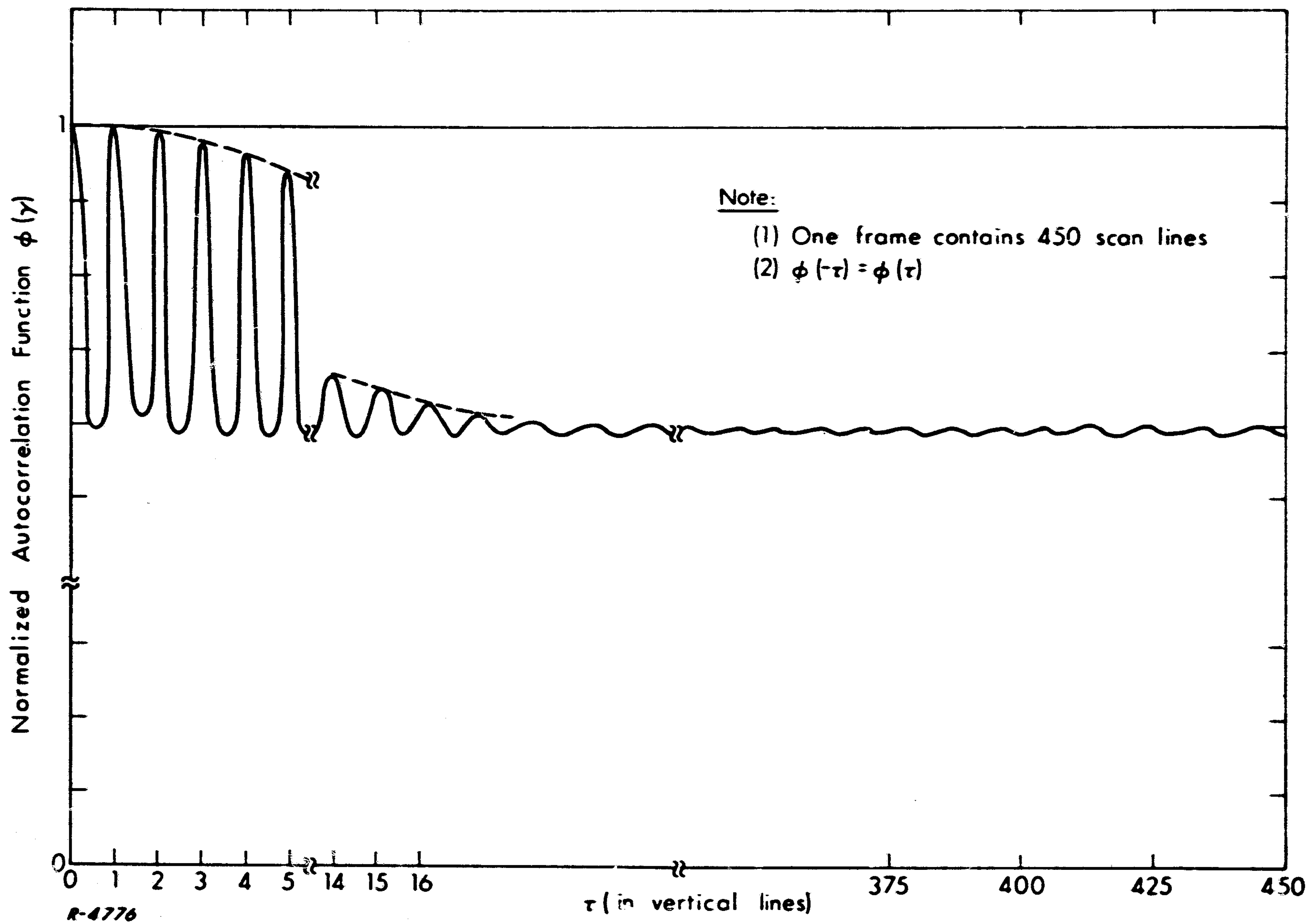

Figure 9 Expected Shape of Normalized Autocorrelation Function For One Frame of Video Data

definition of a normalized correlation coefficient would be

$$\rho(\tau) = \frac{E\{[x(t)-\mu]\cdot[x(t+\tau)-\mu]\}}{\sigma^2} \tag{23}$$

where the division by σ^2 normalizes to unit amplitude at $\tau = 0$.

By expanding Eq. (23) and using Eq. (20) and Eq. (22) it is an easy matter to related $\rho(\tau)$ and $\Phi(\tau)$:

$$\rho(\tau) = \frac{R(\tau)-\mu^2}{\sigma^2} = \frac{(u^2+\sigma^2)\cdot\Phi(\tau)}{\sigma^2} - \frac{\mu^2}{\sigma^2} \tag{24}$$

One recognizes from Eq. (24) above that when $\rho(\tau) = 0$, $\Phi(\tau) = \mu^2/(\sigma^2+\mu^2)$, the nonzero value corresponding to statistically uncorrelated data. $\rho(\tau)$ and $\Phi(\tau)$ are linearly related; hence the former is easily obtainable from the latter. It is only necessary to find the zero level for the $\rho(\tau)$ curve and then adjust the vertical scale so that $\rho(0) = 1$. The shape of the $\rho(\tau)$ curve is the same as the shape of the $\Phi(\tau)$ curve.

Figure 10 shows the $\rho(\tau)$ curve corresponding to one of the $\Phi(\tau)$ curves in Fig. 8. The zero level for $\rho(\tau)$ was obtained by graphically estimating the mean value of $\Psi(\tau)$ in the vicinity of half a line separation. (In cases where computed values of μ and σ are available, this step may be done by calculation.)

If the power spectrum of the video waveform is known, the rms aliasing error, a measure of distortion due to undersampling, can be calculated from the following definition.

$$V_\epsilon = \left\{\frac{\int_{f_s/2}^{\infty} G^2(f)\,df}{\int_0^{\infty} G^2(f)\,df}\right\}^{1/2} \tag{25}$$

where

$G^2(f)$ = the power spectral density; and

f_s = sampling rate.

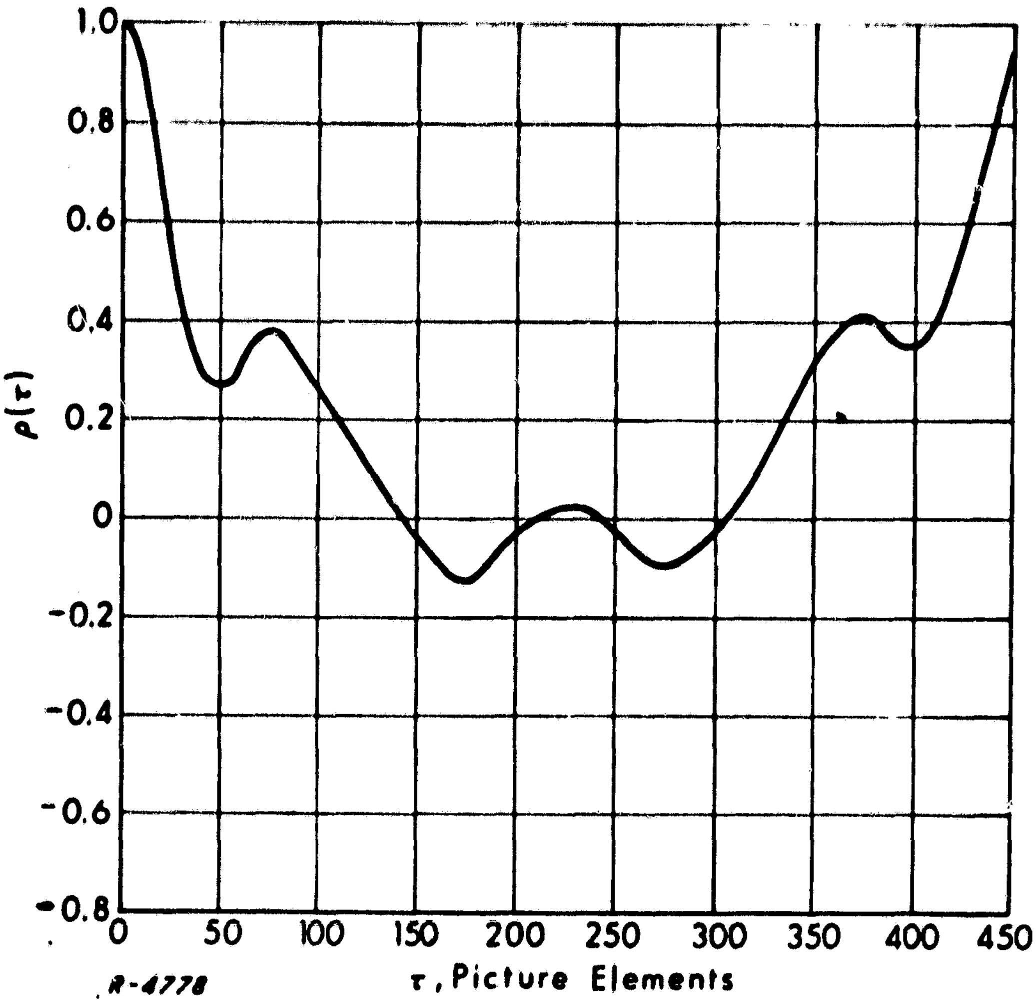

Figure 10 Normalized Correlation Coefficient $\rho(\tau)$ for Picture Segment Data

Equation (25) above expresses the fact that sampling at the rate of f_s samples per second allows the distortionless reproduction of a waveform having no energy above $f_s/2$ Hz. If a process has been under-sampled, i.e., significant energy exists above $f_s/2$, the reconstruction process will "fold over" this energy into the band below $f_s/2$. Serious distortion may thereby be introduced.

Suppose that the signal power spectrum has a Gaussian shape:

$$G^2(f) = \frac{1}{\sqrt{2\pi}\,\sigma} e^{-f^2/2\sigma^2} \tag{26}$$

Furthermore, assume that the sampling rate is such that $f_s/2 = 2.5\sigma$, a point at which the magnitude of $G^2(f)$ is only 0.044 of its dc value. Then

$$\int_{f_s/2}^{\infty} G^2(f)\, df = 0.0062 \tag{27}$$

and

$$\int_0^{\infty} G^2(f)\, df = 0.5 \tag{28}$$

Therefore, the RMS aliasing error is

$$V_\epsilon = \sqrt{\frac{62 \times 10^{-4}}{0.5}} = 0.11 \approx 7 \text{ gray shades!}$$

obviously the power spectrum components above $f = 2.5\sigma$ must be attenuated by filtering if the aliasing error in this example is to be reduced to a tolerable level.

Analysis of Data Waveform Sensitivy to Systematic Errors

Errors introduced into data y physical systems can be divided into two major classes: systematic errors and random errors. Systematic errors are caused by such system imperfections as offset, sensitivity change, non-linearity and non-uniform frequency or phase response. Random errors are primarily the result of random noise perturbations. In this section effects of offset, gain change and gain non-linearity will be analyzed in terms of previously specified Fidelity Criteria. (Ref. 1) Examples are included for selected waveforms.

Figure 11 illustrates the error introduced by offset (a_o) and gain change (a_1). The lower curve of Fig. 11 illustrates the difference (error) between the ideal output (y_I) and the actual output (y_a) as a function of the input voltage (x). The data waveform voltage x varies as a function of time:

$$x = f(t) \tag{29}$$

and thus:

$$e(t) = a_o + a_1 f(t) \tag{30}$$

The time-average error (TAE) is represented by the following:

$$TAE = \frac{1}{T} \int_o^T e(t)\,dt \tag{31}$$

where T is the averaging period. By direct substitution,

$$TAE = \frac{a_o}{T} \int_o^T dt + \frac{a_1}{T} \int_o^T f(t)\,dt \tag{32}$$

Defining the time-average (mean) value of input data voltage as

$$\bar{x} = \frac{1}{T} \int_o^T f(t)dt, \quad \text{TAE becomes:}$$

$$TAE = a_o + a_1 \bar{x} \tag{33}$$

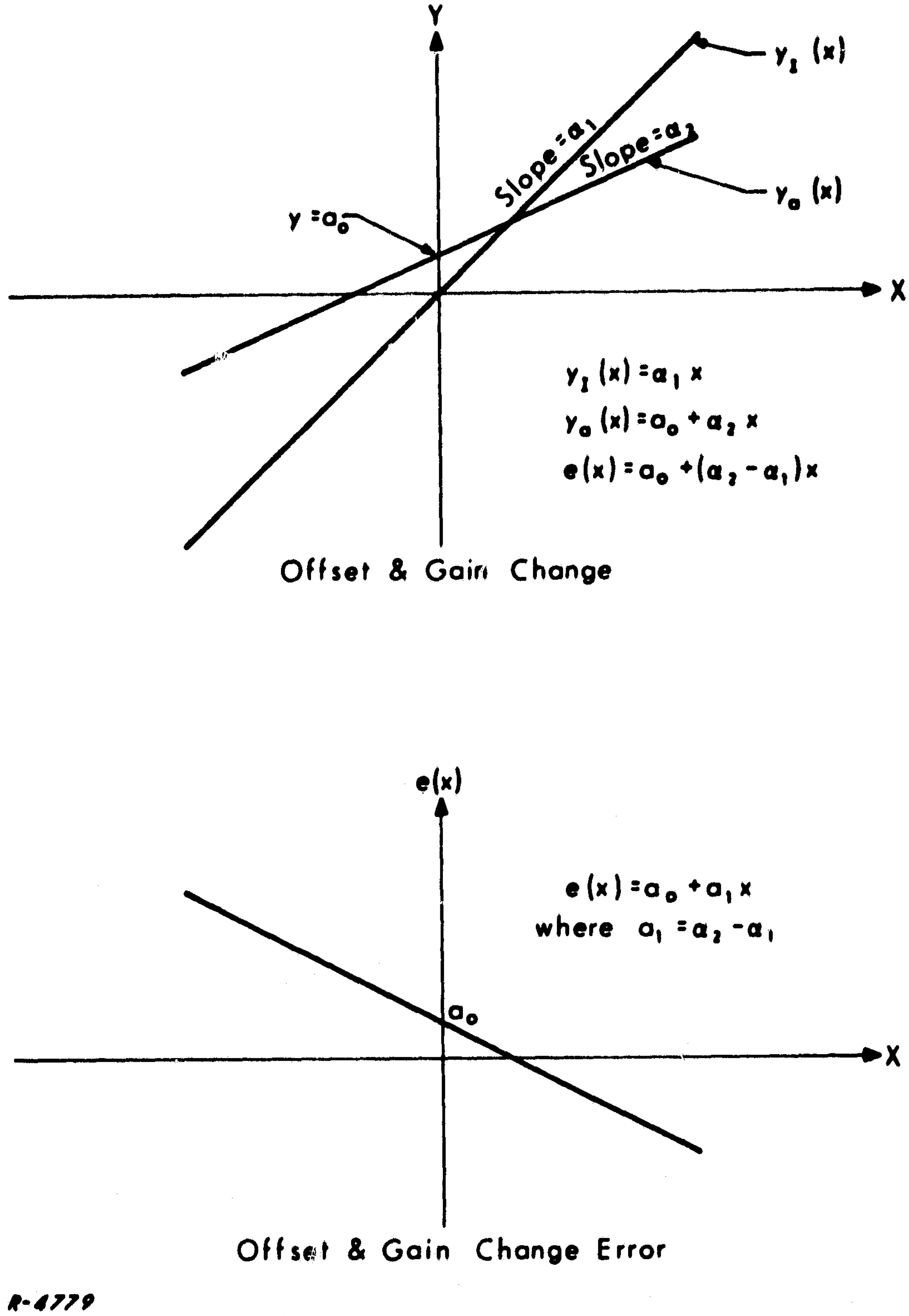

Figure 11 Effect of Offset Gain Change

The time-average squared error (TASE) is defined in the following manner:

$$\text{TASE} = \frac{1}{T} \int_0^T e^2(t)\, dt \tag{34}$$

Substitution of Eq. (30 into Eq. (34) yields the following result:

$$\begin{aligned} \text{TASE} &= \frac{1}{T} \int_0^T \left[a_o^2 + 2\, a_o a_1 f(t) + a_1^2 f^2(t) \right] dt \\ &= a_o^2 + 2 a_o a_1 \overline{x} + a_1^2 \overline{x^2} \end{aligned} \tag{35}$$

where $\overline{x^2}$ is the mean square data value:

$$\overline{x^2} = \frac{1}{T} \int_0^T f^2(t)\, dt \tag{36}$$

The root time-average square error (RTASE) is given by

$$\text{RTASE} = \left[a_o^2 + 2 a_o a_1 \overline{x} + a_1^2 \overline{x^2} \right]^{1/2} \tag{37}$$

Figure 12 illustrates the error introduced by offset (a_o), gain change (a_1) and second degree non-linearities (a_2). In this case e(t) assumes the following form.

$$e(t) = a_o + a_1 f(t) + a_2 f^2(t) \tag{38}$$

It now works out that:

$$\text{TAE} = a_o + a_1 \overline{x} + a_2 \overline{x^2} \tag{39}$$

$$\begin{aligned} \text{TASE} = a_o^2 &+ 2 a_o a_1 \overline{x} + (a_1^2 + 2 a_o a_2) \overline{x^2} \\ &+ 2 a_1 a_2 \overline{x^3} + a_2^2 \overline{x^4} \end{aligned} \tag{40}$$

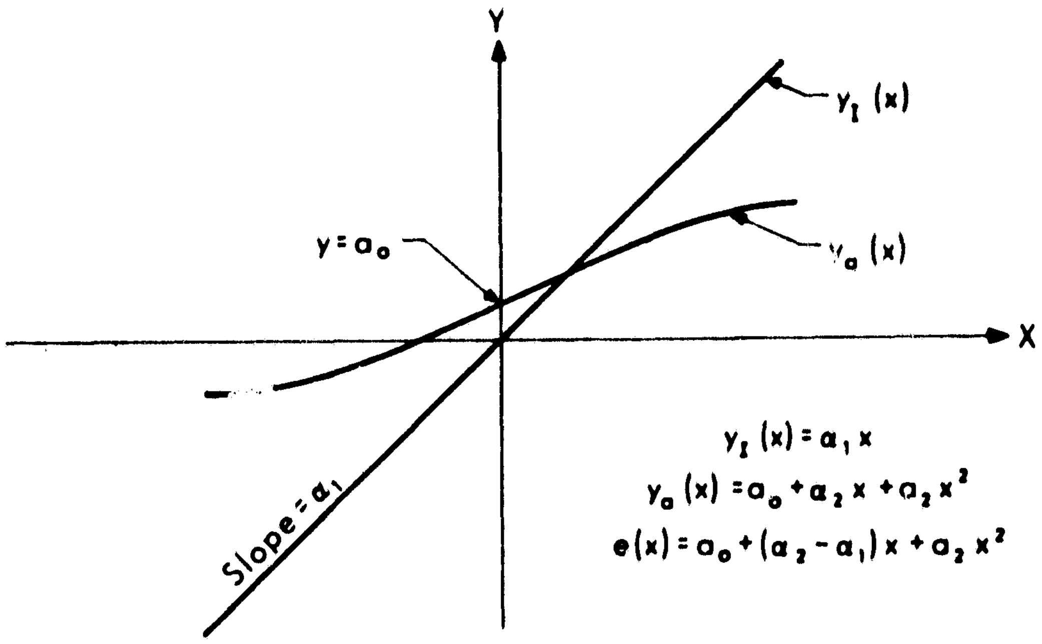

Offset, Gain Change & Second Degree Nonlinearity

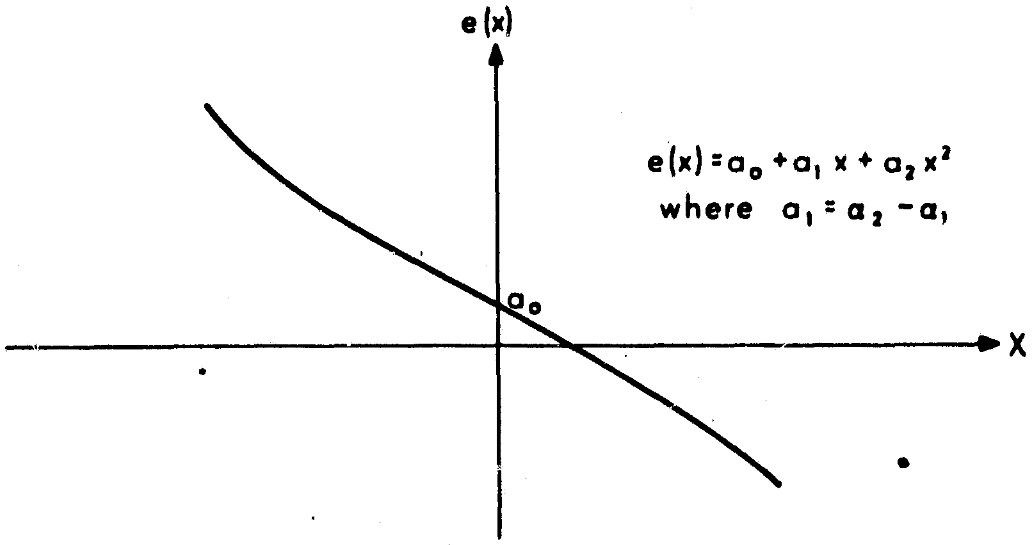

Offset, Gain Change & Nonlinearity Error

R-4780

Figure 12 Effect of Offset, Gain Change and Second Degree Nonlinearity

$$\text{RTASE} = \left[a_o^2 + 2a_o a_1 \overline{x} + (a_1^2 + 2a_o a_2 \overline{x^2}) + 2a_1 a_2 \overline{x^3} + a_2^2 \overline{x^4} \right]^{1/2} \tag{41}$$

where $\overline{x^3}$ and $\overline{x^4}$ denote the time-average values of x^3 and x^4.

The above results will be applied to the four following basic waveform types to study their relative sensitivity to systematic errors: Sinusoidal wave, exponentially decaying wave, sawtooth wave, and square wave. The waveforms may all be thought of as repetive cycles of the basic waveshape. All time-averaged values are calculated on the basis of a whole waveform cycle; the identical time-averaged values would hold for any integral number of cycles.

The four waveforms are defined as follows. For each the defined first full cycle continues to repeat itself.

Sinusoidal data:

$$f_1(t) = \frac{1}{2} (1 + \cos t) \qquad 0 \le t \le 2\pi \tag{42}$$

$$f_1(t+2n\pi) = f_1(t) \qquad n = 1, 2, \ldots$$

$$\overline{x} = 1/2, \ \overline{x^2} = 3/8$$

Exponential data:

$$f_2(t) = e^{-t/\tau} \qquad 0 \le t \le 5\tau \tag{43}$$

$$f_2(t+5n\tau) = f_2(t) \quad n = 1, 2, \ldots$$

$$\overline{x} = 0.199 \qquad \overline{x^2} = 0.100$$

Sawtooth data:

$$f_3(t) = t \qquad 0 \le t \le 1 \tag{44}$$

$$f_3(t+n) = f_3(t) \quad n = 1, 2, \ldots$$

$$\overline{x} = 1/2 \qquad \overline{x^2} = 1/3$$

Square Wave data:

$$f(t) = \begin{cases} 1 & 0 \le t \le \tau/2 \\ 0 & \tau/2 \le t \le \tau \end{cases} \qquad (45)$$

$$f(t + n\tau) = f(t) \qquad n = 1, 2, \ldots$$

$$\bar{x} = 1/2 \qquad \overline{x^2} = 1/2$$

It is first assumed that zero offset and gain change represent the only systematic error sources. We further let $a_o = 0.005$ and $\alpha_2 = 0.95$:

$$y_a(x) = 0.005 + 0.95x \qquad (46)$$

The evaluations of time-average error (TAE) root time-average square error (RTASE), and maximum absolute error (MAE) were carried out by using $a_o = 0.005$, $a_1 = -0.05$ in Eqs. (33) and (37). The results, expressed as a percentage of full scale value, are presented as Table 1.

Table 1

Systematic Errors Due to Offset and Gain Changes

$$e(t) = 0.005 - 0.05f(t)$$

	TAE(% of f. s.)	RTASE(% of f. s.)	MAE(% of f. s.)
	-2%	2.67%	4.5%
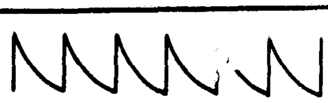	-0.5%	1.33%	4.5%
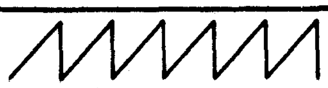	-2%	2.47%	4.5%
	-2%	3.2%	4.5%

For the second set of examples assume that the circuit transfer function has a second order non-linearity in addition to the zero offset and gain change. Furthermore assume values of $a_o = 0.005$, $\alpha_2 = 1.1$ and $a_2 = -0.1$; i.e.,

$$y_a(x) = 0.005 + 1.1x - 0.1x^2. \qquad (47)$$

Then,

$$e(t) = 0.005 + 0.1f(t) - 0.1f^2(t). \tag{48}$$

The determination of the data errors generated in subjecting the four waveforms to this non-linearity model is summarized in Table II.

Table II

Systematic Errors Due to Offset, Gain Change and Nonlinearity

$$e(t) = 0.005 + 0.1f(t) - 0.1f^2(t)$$

	TAE(%of f. s.)	RTASE(%of f. s.)	MAE(%of f. s.)
	1.75%	1.98%	3%
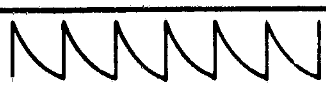	1.5%	1.71%	3%
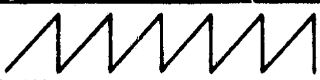	2.17%	2.3%	3%
	0.5%	0.5%	0.5%

Summary of Performance of Compression Algorithms

During the course of this effort,picture compression simulations have been performed employing the following compression algorithms: Zero Order Predictor (ZOP),Zero Order Interpolator (ZOI), First Order Interpolator, Disjoined Line Segments (FOIDIS), First Order Interpolator, Out of Tolerance (FOIOOT), Second Order Interpolator, Disjoined (SOIDIS), and Second Order Interpolator, Out of Tolerance, (SOIOOT).

As described in greater detail in Ref. 1, SOIDIS attempts to fit a parabola through a sequence of data waveform sample values such that the parabola

1. passes through the first data point;
2. passes no more than a certain prespecified distance (the tolerance) away from from each succeeding data point; and
3. continues in this fashion for as many data points as possible.

The constructed parabola thus represents the first m data samples to the required fidelity; a new parabola is initiated with the m + 1st data point and carried on as far as possible in the same manner. SOIOOT operation differs in that the beginning value of the new parabola segment is equal to the termination value of the old segment plus or minus a fixed displacement as given by a single (out-of-tolerance) bit. This stands in contrast to the six bits required to describe the starting point of the new SOIDIS parabola in the 64 level gray scale quantization employed in this study.

FOIDIS and FOIOOT operate in an analogous manner, fitting the data with straight line segments. ZOI fits the data with a horizontal line segment "staircase" approximation; the amplitude of each horizontal line segment is selected to fit the longest possible run of data samples. ZOP initiates a horizontal line at a sample value. It is continued for as many samples as it describes within tolerance. The first sample value not representable by this horizontal line initiates a new horizontal line.

Compression algorithm performance is usually described in terms of the line-segment compression ratio or the bit compression ratio produced by the processing of a given specimen of data.

Line segment compression ratio is defined as follows:

$$\overline{N} = \frac{\text{\# of sample points processed}}{\text{\# of line segments required}} \qquad (49)$$

where the term "line segment" is understood to signify a segment of a parabola when reference is to the SOI. The second order interpolation algorithm necessarily produces line segment compression ratios which are at least as high as the compression ratios resulting from first order interpolation. This conclusion arises from the fact that the straight line is merely a subclass of the parabola with one parameter (the curvature) constrained to zero. Thus FOI is a special case of SOI. No general statement can be made, a priori, concerning the relative efficiency (in terms of bandwidth compression capability) of FOI and SOI compression algorithms, since bandwidth compression achieved depends not only on line segment compression ratio achieved, but also on the amount of information required to characterize each line segment. Thus bandwidth (bit) compression ratio may be defined in the following manner.

$$\overline{N_b} \equiv \overline{N} \left\{ \frac{\text{\# of bits/processed sample point}}{\text{\# of bits/line segment required}} \right\} \qquad (50)$$

SOI obviously requires more information per line segment than does FOI. Consequently in some instances FOI may be more efficient than SOI simply because the superior line segment compression ratio achieved by SOI may not be sufficient to offset the increased amount of data needed to specify a line segment relative to FOI.

Line segment compression ratios obtained by compressing a portion of a high resolution reconnaisance photo with different algorithms are presented in Fig. 13. Results are for a 64 level (6 bit) quantization gray scale. Minor variations between some ratios contained herein and their counterparts quoted in Ref. 1 are due to the use of a narrower section of picture in the earlier work to achieve usable results more economically.

Observe that both the ZOP and ZOI algorithms require eleven transmitted data bits per required line segment: six bits for data magnitude and five bits for line segment (run) length. Thus, for ZOI or ZOP the average bandwidth compression ratio becomes;

$$\overline{N_b} = \left(\frac{6}{11}\right)\overline{N}. \qquad \text{(ZOP and ZOI)} \qquad (51)$$

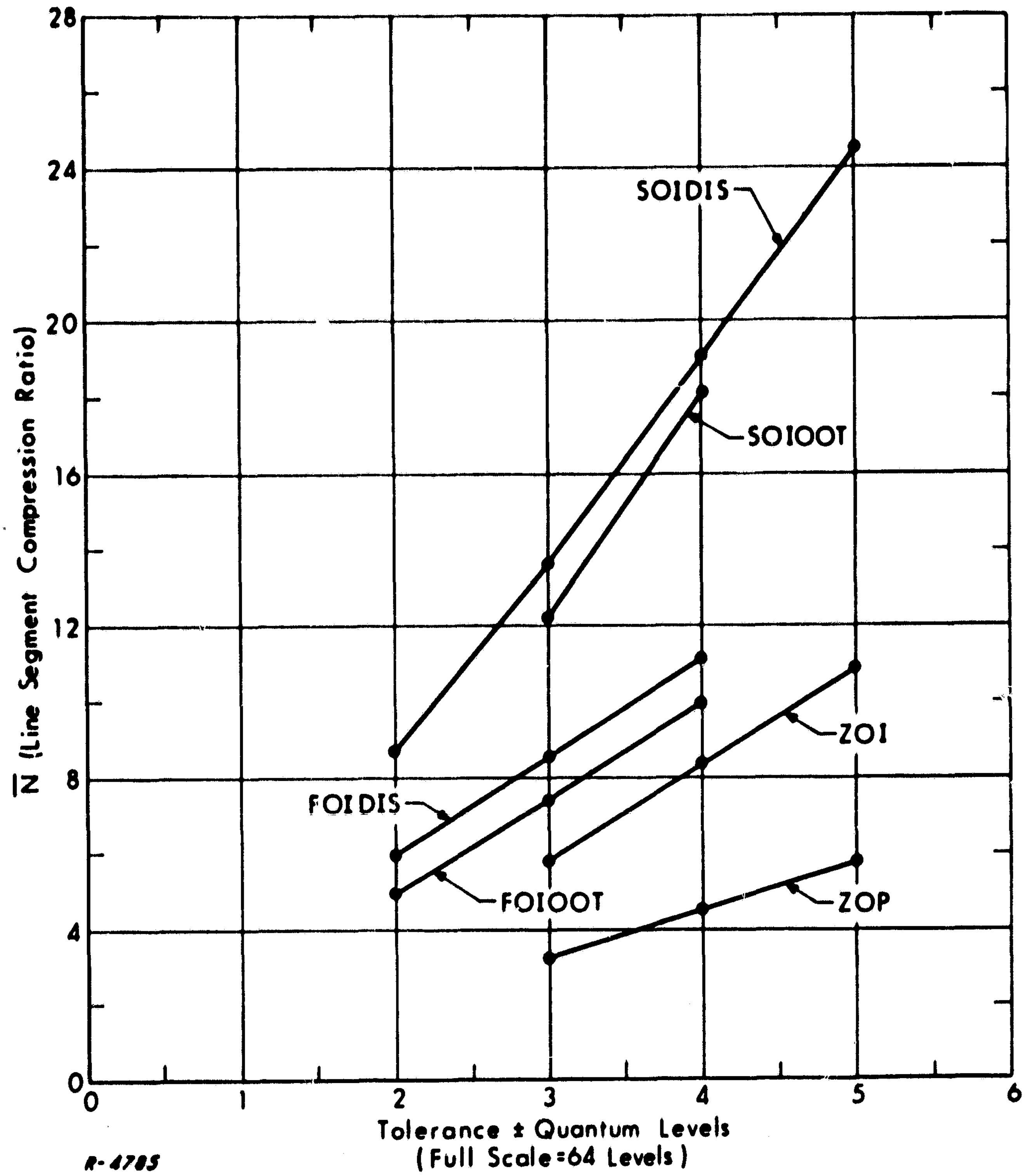

Figure 13 Performance of Compression Algorithms on Segment of High Resolution Reconnaissance Photo (Line Segment Compression Ratio)

The FOIDIS algorithm requires the transmission of 17 bits per line segment; six bits are needed to specify data magnitude of the initial point, six bits for data magnitude of the end point, and five bits for run length. Thus the FOIDIS bandwidth compression ratio may be expressed as follows.

$$\overline{N_b} = \left(\frac{6}{17}\right) \overline{N} \qquad \text{(FOIDIS)} \qquad (52)$$

The FOIOOT algorithm requires the transmission of 12 bits per line segment; one bit specifies direction (+ or -) of offset of the initial point from the end point of the preceding segment, six bits specify data magnitude of the end point and five bits specify run length. The FOIOOT bandwidth compression ratio may be expressed as follows.

$$\overline{N_b} = \overline{N}/2 \qquad \text{(FOIOOT)} \qquad (53)$$

The number of bits required for specification of SOIDIS and SOIOOT "line" segments was an unknown quantity prior to this study, in contrast to the case for the preceding algorithms. Therefore a digression is required to define the coding technique from which average bit compression ratios were computed.

The SOI algorithm is based on the determination of coefficients a, b, and c describing an approximating parabola.

$$\hat{y}_n = an^2 + bn + c \qquad n = 0, 1, 2, \ldots \qquad (54)$$

where $\hat{y}_n$ is the value of the parabola corresponding to the n^{th} sample time. The coefficients are chosen to maximize the run length for a given error tolerance (maximum permissible error between $\hat{y}_n$ and the true value y_n). They must be specified to a sufficient number of significant bits to assure that $|y_n^* - \hat{y}_n|$ does not exceed half of a quantum level (1/128 of full scale), where,

$$y_n^* = a^*n^2 + b^*n + c^* \qquad (55)$$

and a*, b*, and c* indicate the transmitted parameter values.

At first glance it appears that a transmitted word should contain the calculated values of a, b, c, and run length. However this most obvious approach is unsatisfactory because of the number of bits required to specify a and b with sufficient accuracy.

The following efficient technique for coding the parabolic segment has been developed. Suppose first that the algorithm has produced (we shall assume with arbitrarily high accuracy) the parameters a, b, and c of the approximating parabola. Then the values of this parabola are calculated at $n = 0$, $n = N/2$, $n = N$, where the parabola approximates a sequence of $N + 1$ samples (i.e., N is the run length). These values are then rounded off to six bits; the three six-bit words plus a five-bit run length word constitute the 23 bits used to transmit a SOIDIS line segment.

The transmitted parabola thus conveys the set of parameters a^*, b^*, c^* which differ by some finite amount from the ideal set a, b, and c. Note that the parameter c, which is identifiable as the initial sample value at $n=0$, must be the same for both the ideal and the transmitted parabola.

One may easily obtain an expression for the error between the two parabolas as a function of n:

$$E(n) = \hat{y}_n - y_n^* = (a - a^*) n^2 + (b - b^*) n \qquad (56)$$

Letting

$$a - a^* \equiv C = \text{error in curvature}$$

and

$$b - b^* \equiv S = \text{error in slope}$$

Eq. (56) above becomes:

$$E(n) = Cn^2 + Sn \qquad (57)$$

The three transmitted data values will have errors given by:

$$E(0) = 0 \qquad (58)$$

$$E(N/2) = \frac{N^2}{4} C + \frac{N}{2} S \qquad (59)$$

$$E(N) = N^2 C + NS \qquad (60)$$

Expressions for C and S can be determined from Eqs. (59) and (60):

$$C = \frac{2E(N) - 4E(N/2)}{N^2} \qquad (61)$$

$$S = \frac{4E(N/2) - E(N)}{N} \qquad (62)$$

Substituting Eqs. (61) and (62) into Eq. (57) yields the following expression for error in the reconstructed line segment at any sample point.

$$E(n) = n^2 \left\{ \frac{2E(N) - 4E(N/2)}{N^2} \right\} - n \left\{ \frac{E(N) - 4E(N/2)}{N} \right\} \tag{63}$$

The sample point which suffers the largest absolute error may be found through differentiation of Eq. (63) and setting the derivative equal to zero. The location of this point n_p only has significance when $0 \leq n_p \leq N$, for it then corresponds to a maximum error within the run of samples represented by the parabola. The point n_p is given by:

$$n_p = \frac{N[E(N) - 4E(N/2)]}{4[E(N) - 2E(N/2)]} \tag{64}$$

The reconstruction error at this point is:

$$E(n_p) = \frac{[4E(N/2) - E(N)]^2}{8[E(N) - 2E(N/2)]} \tag{65}$$

The transmission of six-bit sample magnitudes constrains the errors at $n = N/2$ and $n = N$ to be less than or equal to one part in 128 (denoted by ϵ). The maximum reconstruction error occurs when

$$E(N) = E(N/2) = \epsilon$$

or

$$E(N) = E(N/2) = -\epsilon.$$

This error will occur at $n_p = 3/4\ N$ with a magnitude of

$$|E(n_p)| = 9\epsilon/8 = \frac{9}{8 \times 128}\ . \tag{66}$$

With small probability the error in the reconstructed parabola may exceed ϵ by an amount which is deemed to be tolerable on account of its infrequent occurrence and small magnitude. Therefore 23 bits per line segment must be transmitted for the SOIDIS algorithm, and the SOIDIS bandwidth compression ratio may be expressed as follows.

$$\overline{N_b} = \frac{6}{23}\overline{N} \qquad \text{(SOIDOS)} \tag{67}$$

The SOIOOT algorithm requires the transmission of 18 bits per line segment; one bit specifies direction (+ or -) of a single tolerance offset of the initial point from the end point of the preceding segment, six bits each are needed to specify data magnitude of the mid-point and end point of the line segment and five bits specify run length. The average SOIOOT bandwidth compression ratio is:

$$\overline{N_b} = \frac{1}{3}\overline{N} \qquad \text{(SOIOOT)} \tag{68}$$

Bandwidth compression ratios as a function of tolerance settings obtained by compressing a portion of the high resolution reconnaissance photo with various algorithms are presented in Fig. 14. Note that the out-of-tolerance algorithms (FOIOOT and SOIOOT) provide greater average bit compression ratios than their disjoint counterparts. This represents a reversal from the curves of line segment compression ratio shown in Fig. 13.

The original reconnaissance photo (after scanning) is shown in Fig. 15. Compressed and reconstructed versions of this photo are illustrated in Figs. 16, 17, 18, and 19 using ZOI, FOIOOT, SOIDIS, and SOIOOT algorithms respectively. Figures 20 and 21 are original photos of the lunar surface provided by the Surveyor I vehicle. FOIOOT compressed and reconstructed versions of these photos are presented in Figs. 22 and 23 respectively. SOIOOT versions are presented in Figs. 24 and 25.

It is of interest to form a comparison of the bandwidth compression ratios achieved by two different algorithms against a series of pictures, as is done below.

Algorithm	$\overline{N_b}$ Achieved on		
	Reconnaisance Photo	Surveyor #1	Surveyor #2
FOIOOT	3.7	6.8	2.9
SOIOOT	4.1	6.4	3.1

The comparison clearly illustrates that the "compressibility" of a picture depends quite strongly upon its subject matter, and that while the absolute performance of a pair of algorithms in a series of pictures will vary considerably their relative performance will show only mild variation.

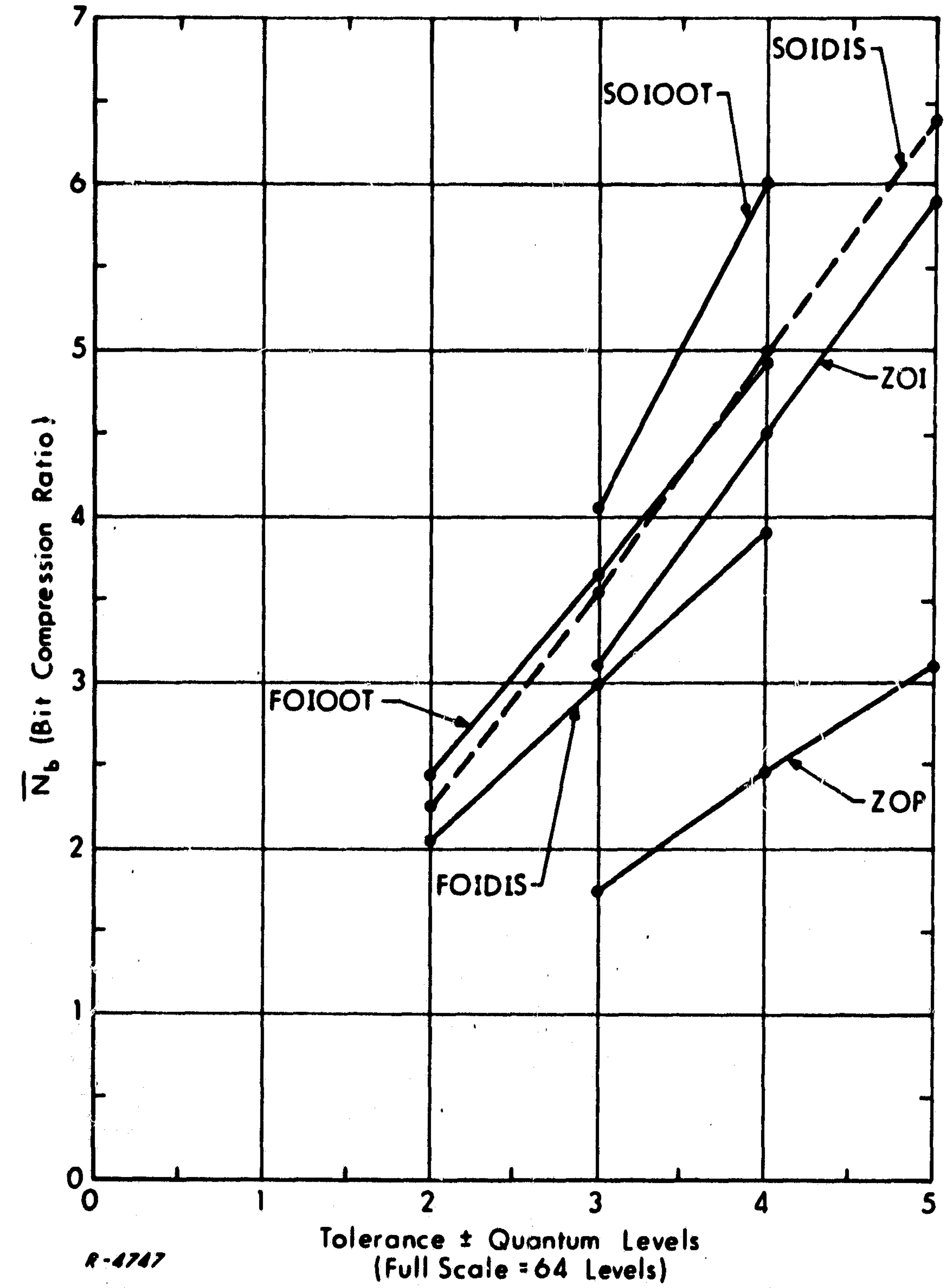

Figure 14 Performance of Compression Algorithms on Segment of High Resolution Reconnaissance Photo (Bit Compression Ratio)

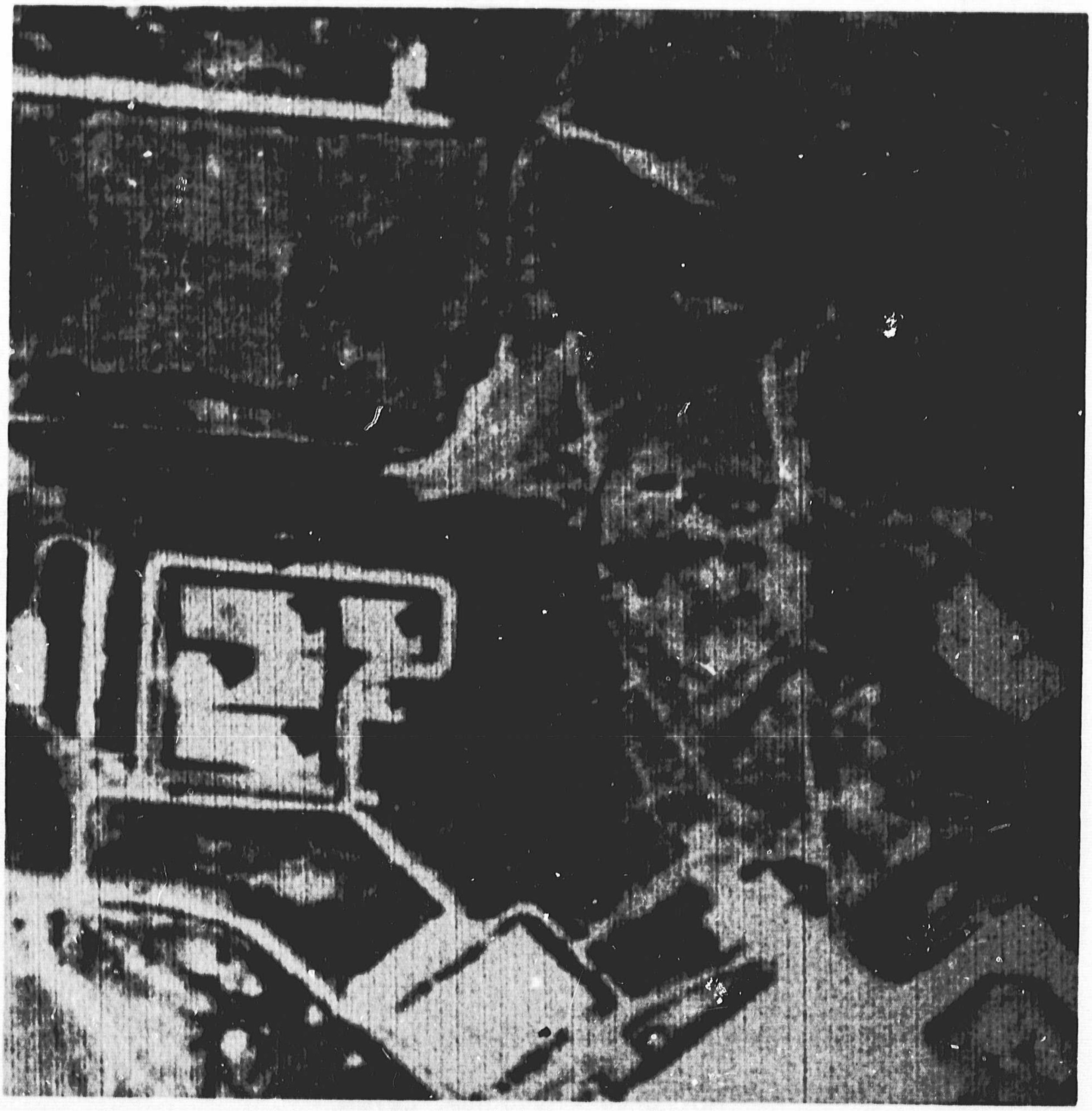

Fig. 15 Original Reconnaissance Photo (Scanned and Reconstructed).

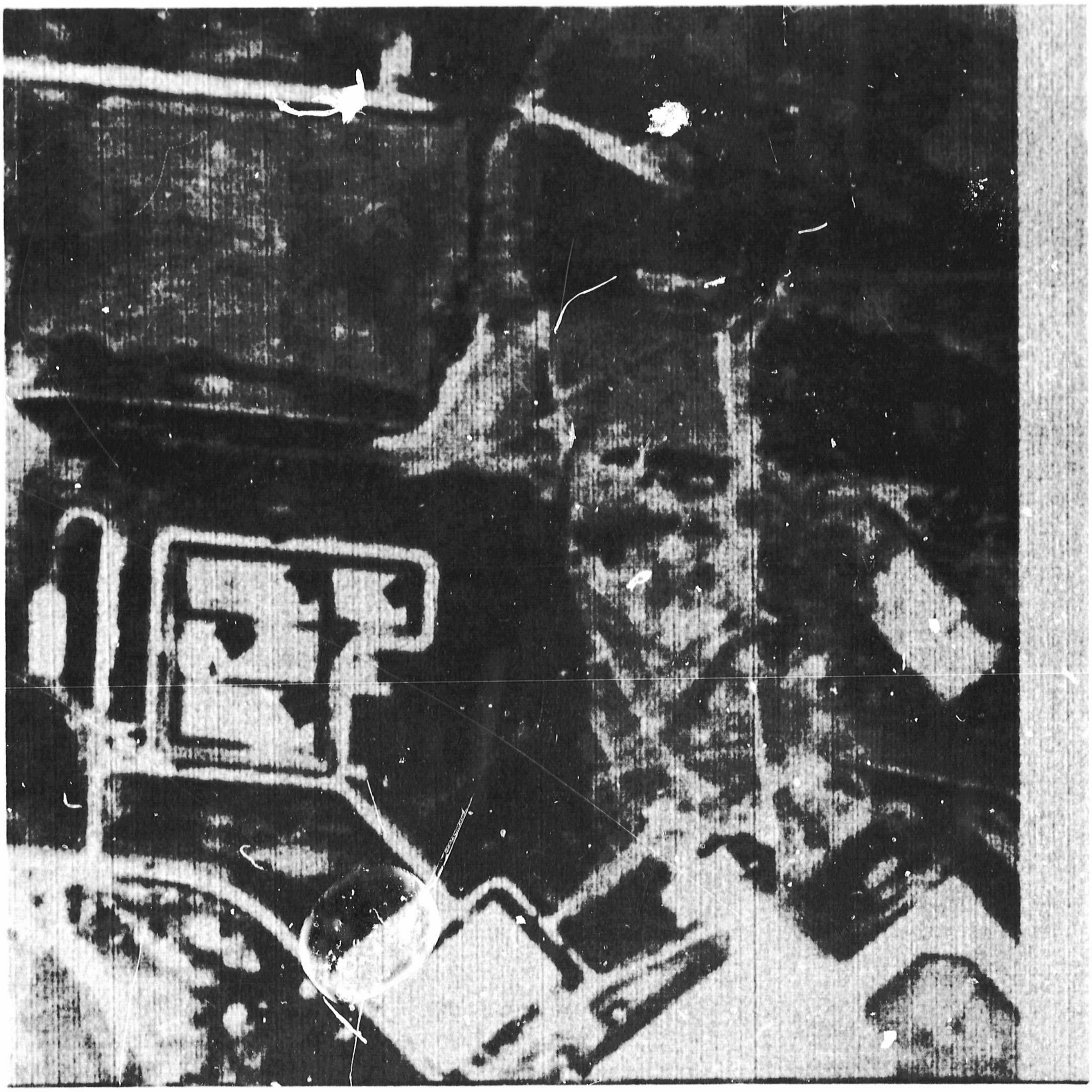

Fig.16 ZOI Compressed Reconnaissance Photo. Tolerance = 3, $\overline{N}$ = 5.77, $\overline{N}_b$ = 3.12.

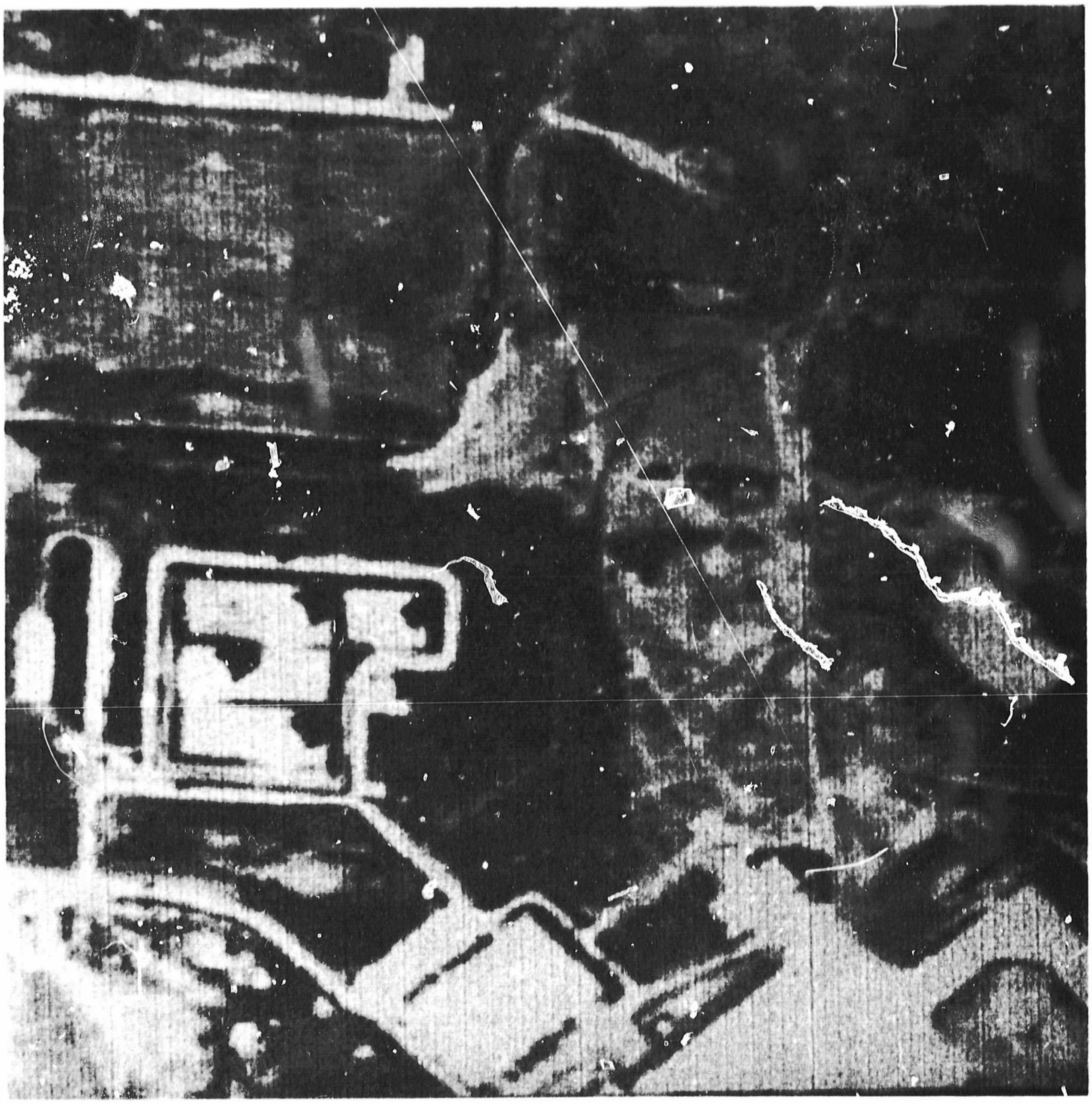

Fig.17 FOIOOT Compressed Reconnaissance Photo.
Tolerance = 3, $\bar{N}$ = 7.4, $\bar{N}_b$ = 3.7.

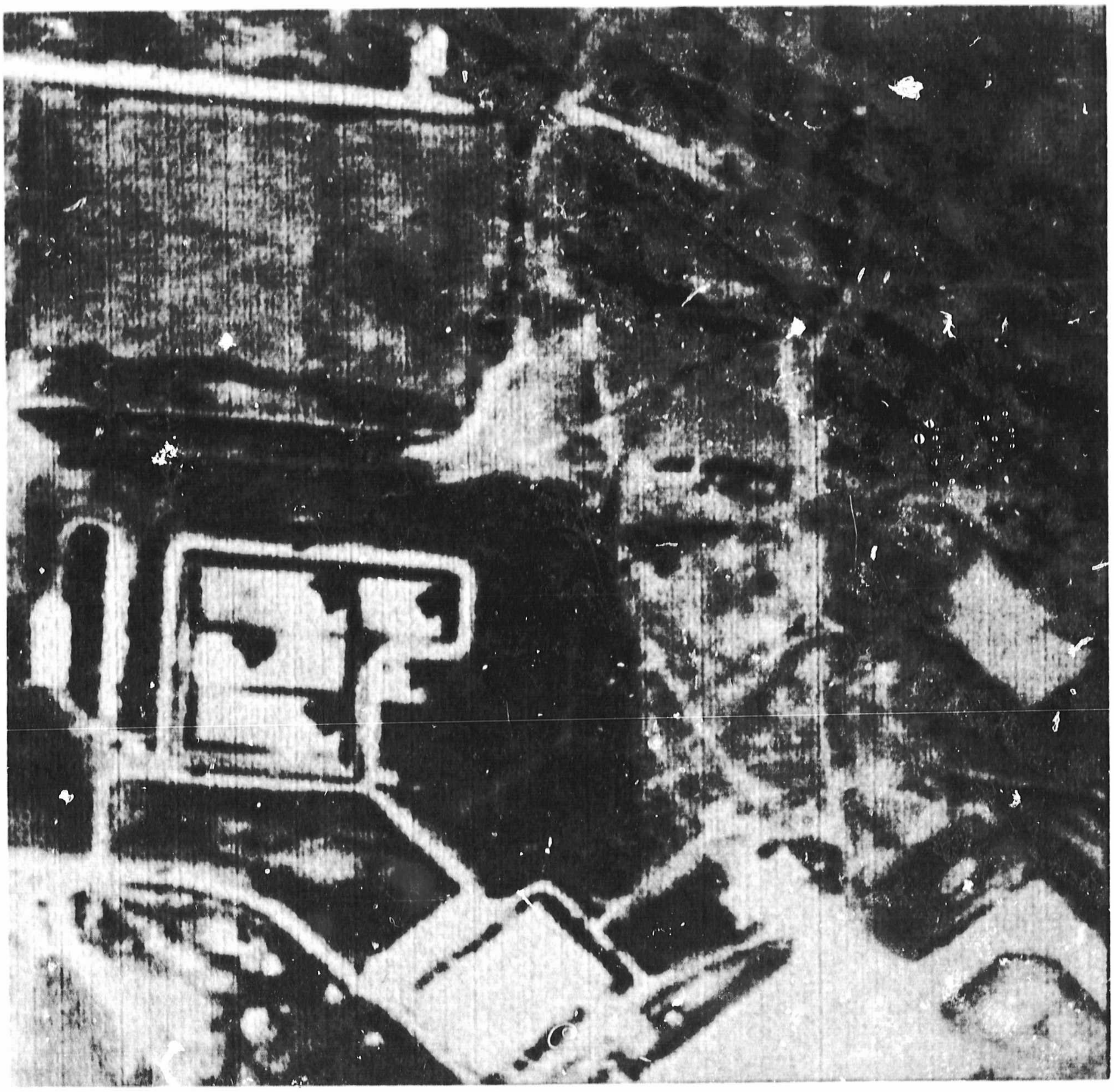

Fig. 18 SOIDIS Compressed Reconnaissance Photo.
Tolerance = 3, $\overline{N}$ = 13.6, $\overline{N}_b$ = 3.55.

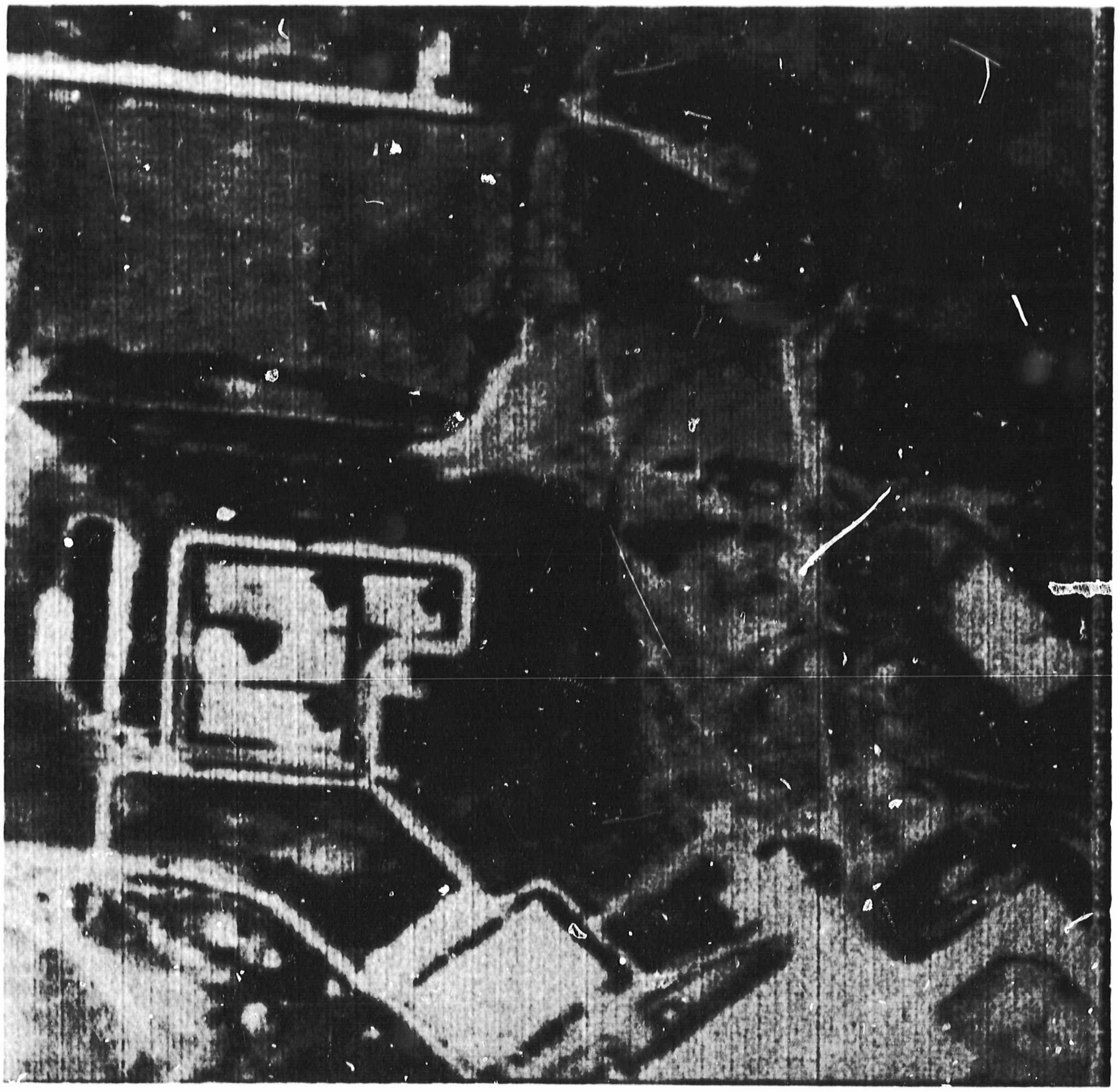

Fig. 19 SOIOOT Compressed Reconnaissance Photo.
Tolerance = 3, $\overline{N}$ = 12.2, $\overline{N}_b$ = 4.1.

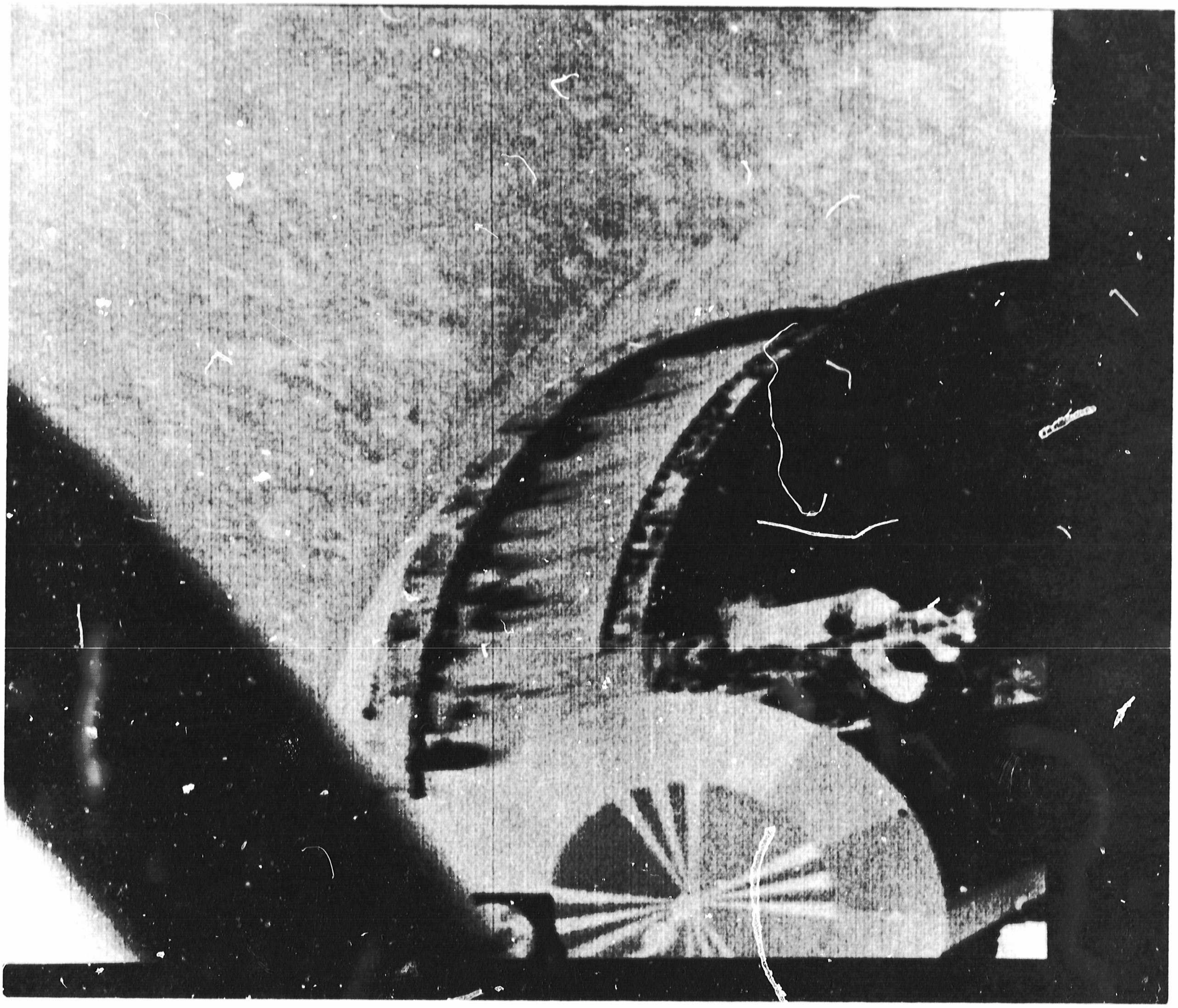

Fig. 20 Original - #1 Surveyor Photo.

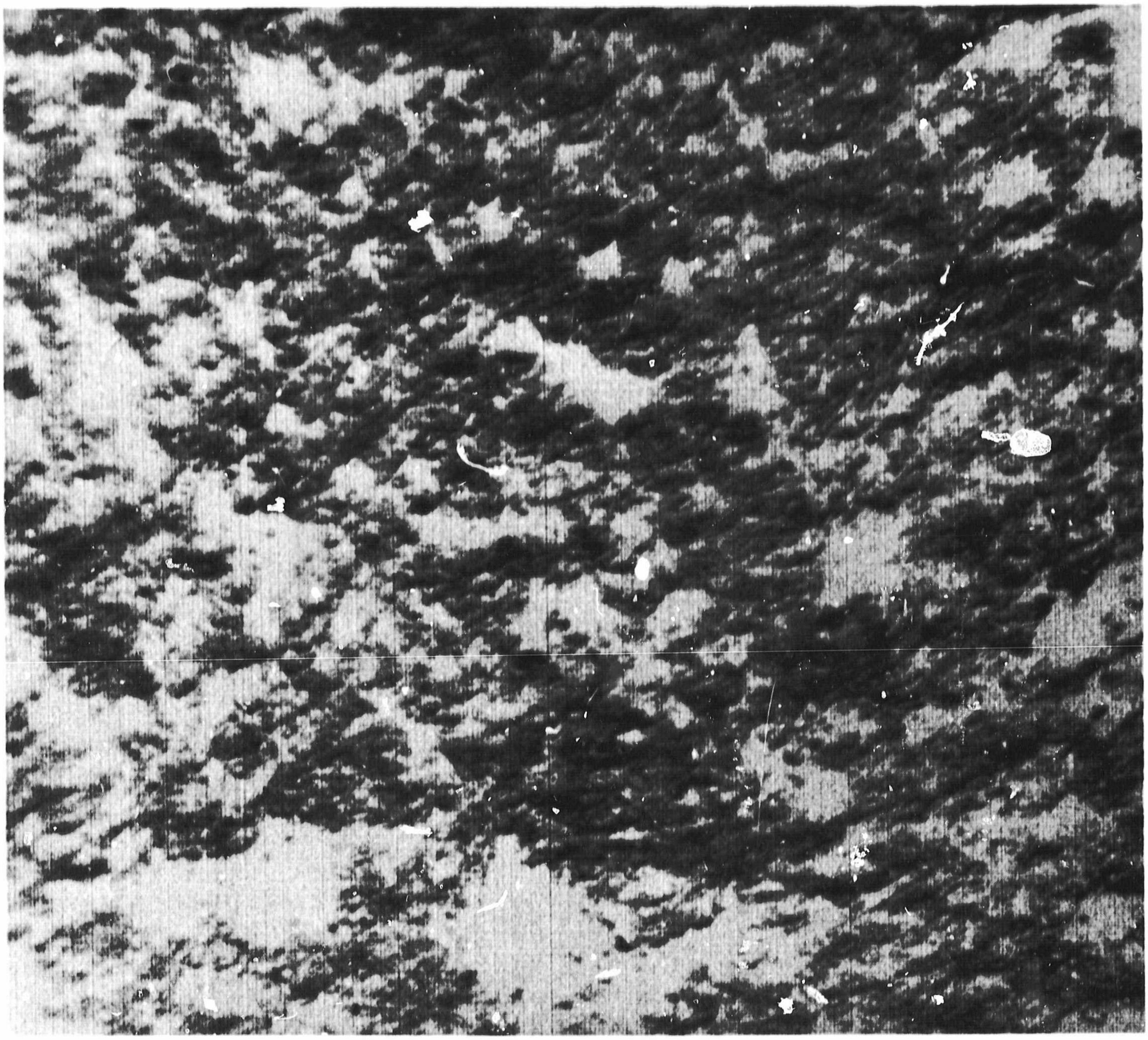

Fig. 21 Original - #2 Surveyor Photo.

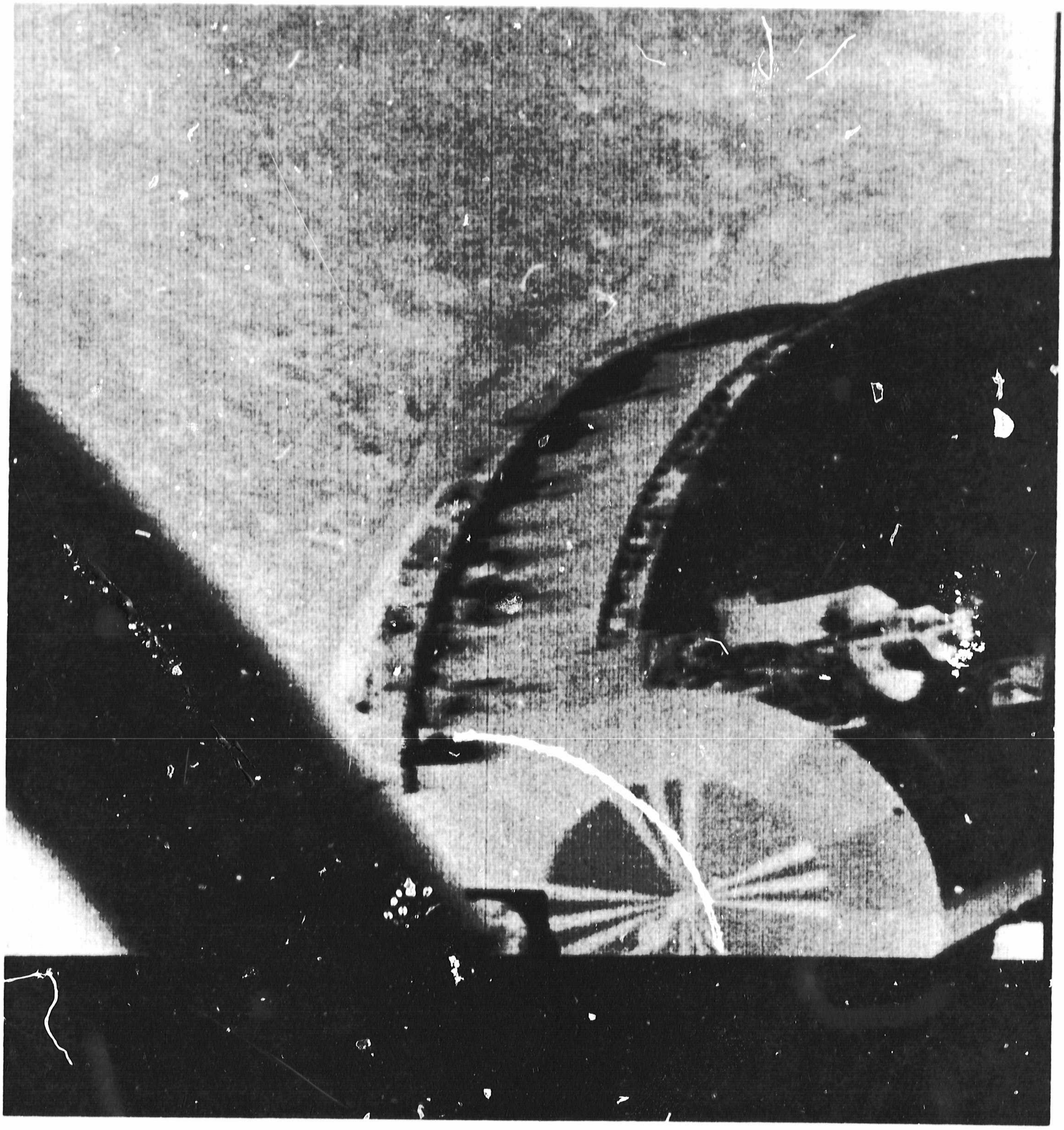

Fig.22 FOIOOT Compressed Surveyor Photo #1
Tolerance = 3, $\overline{N}$ = 13.7, $\overline{N}_b$ = 6.85.

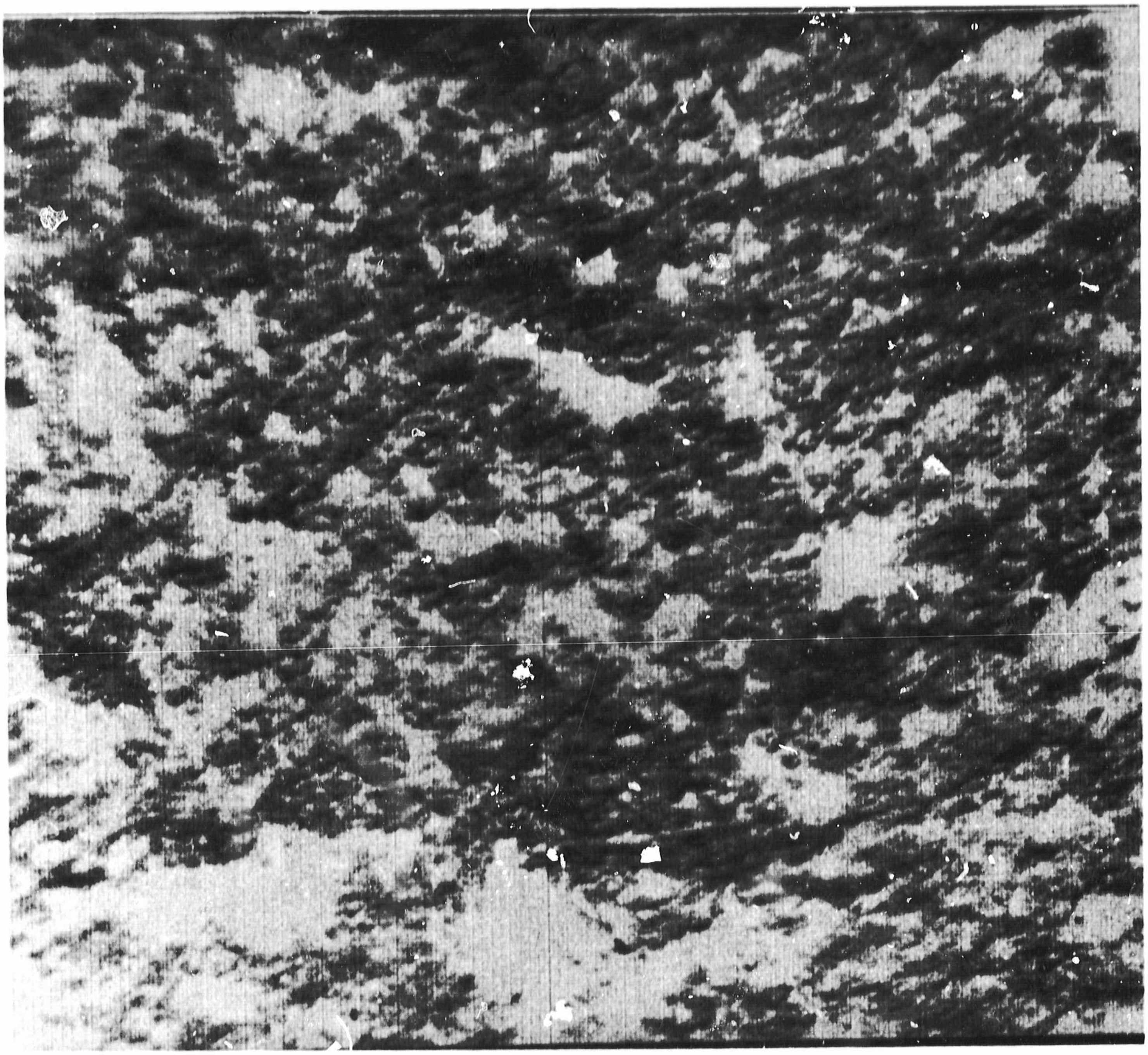

Fig.23 FOIOOT Compressed Surveyor Photo #2
Tolerance = 3, $\overline{N} = 5.77$, $\overline{N}_b = 2.89$

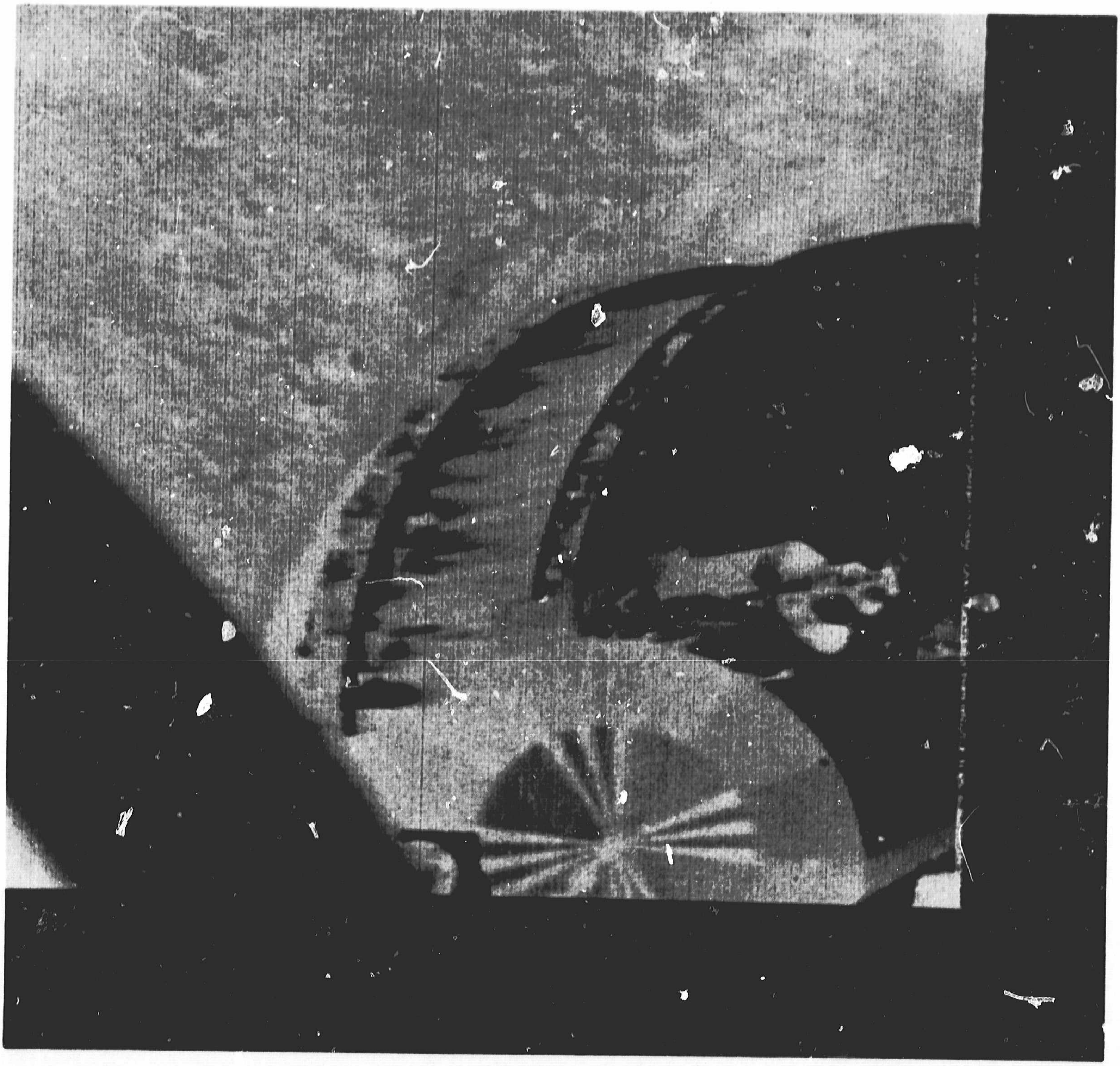

Fig.24 SOIOOT Compressed Surveyor Photo #1
Tolerance = 3, $\overline{N} = 19.27$, $\overline{N}_b = 6.42$.

#2

Fig.25 SOIOOT Compressed Surveyer Photo #2
Tolerance = 3, $\overline{N} = 9.23$, $\overline{N}_b = 3.08$.

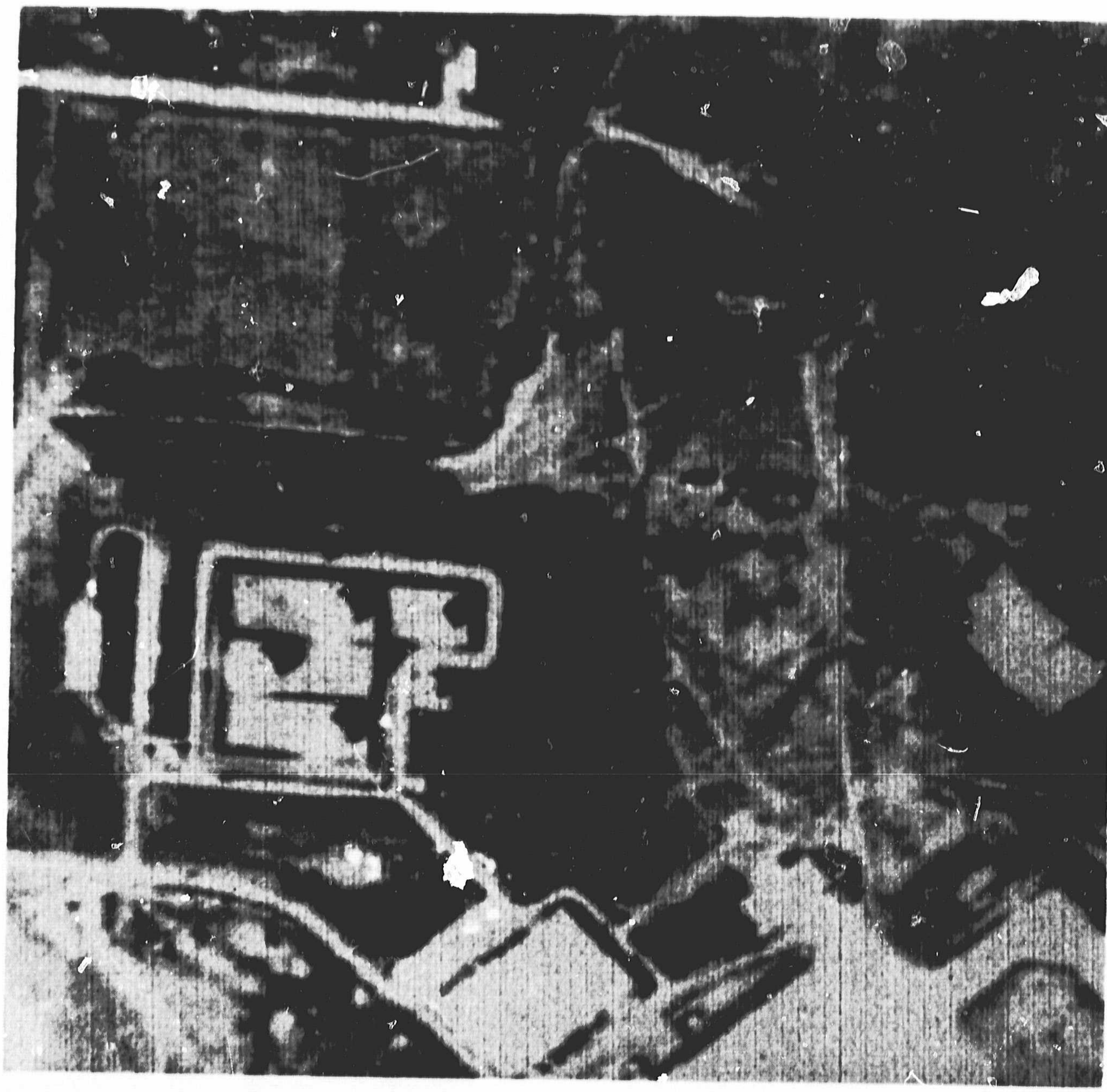

Fig. 26 Reconnaissance Photo, Noisy PCM, 10^{-3} Bit Error Probability.

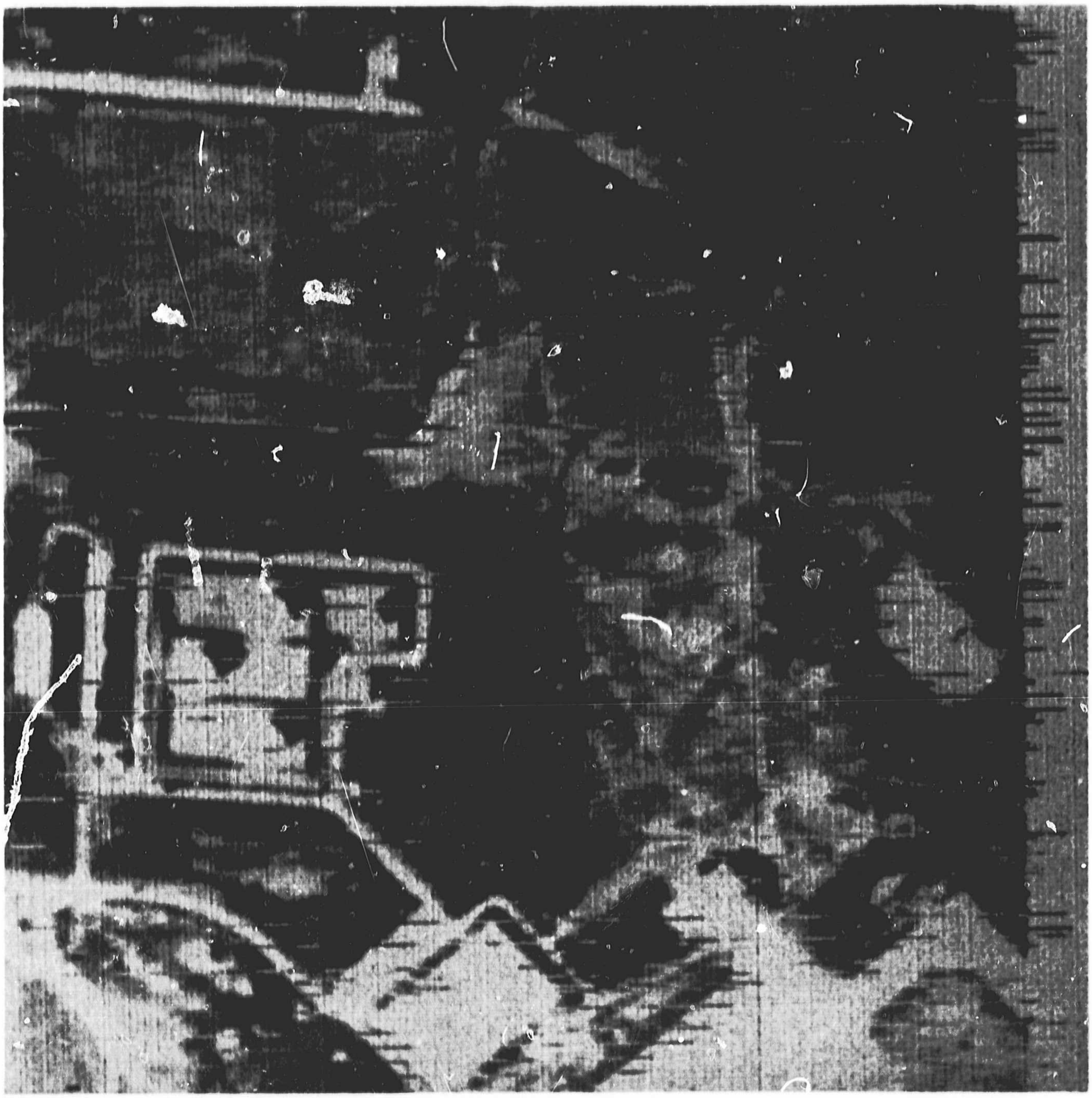

Fig. 27 ZOI Compressed Reconnaisance Photo, 10^{-3} Bit Error Probability No Error Control. (Tolerance = 3, $\overline{N}$ = 5.77, $\overline{N}_b$ = 3.12)

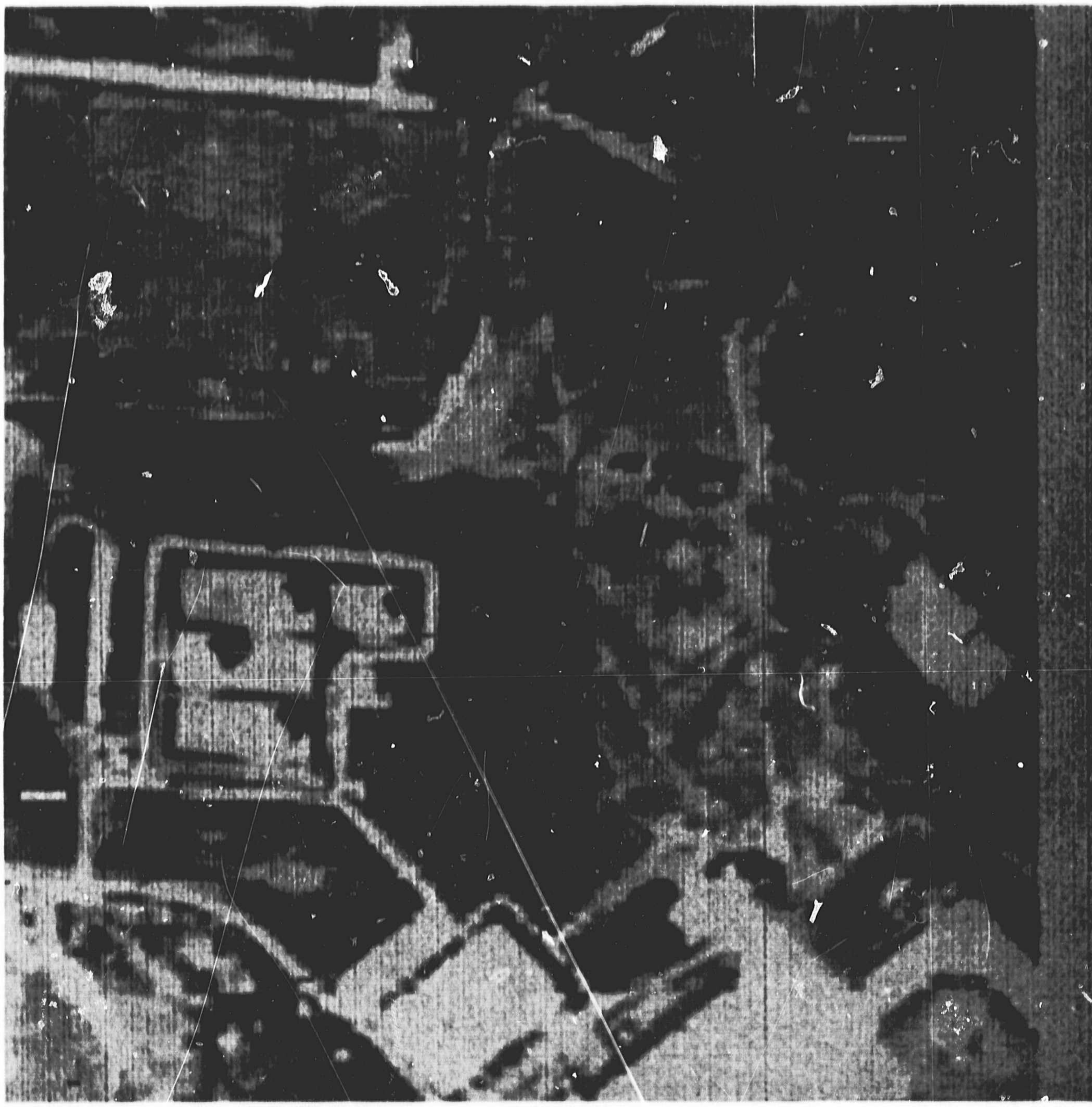

Fig. 28 ZOI Compressed Reconnaissance Photo, 10^{-3} Bit Error Probabili
Line Substitution Error Control, Allowance Value $\alpha = 0$.
(Tolerance = 3, $\overline{N} = 5.77$, $\overline{N}_b = 3.12$)

Fig. 29 FOIOOT Compressed Reconnaissance Photo, Bit Error Probability = 10^{-3}, No Error Control. (Tolerance = 3, $\overline{N} = 7.4$, $\overline{N}_b = 3.7$)

Fig. 30 FOIOOT Compressed Reconnaissance Photo Bit Error Probability = 10^{-3}, Line Substitution Error Control Allowance Value α = 0. (Tolerance = 3, $\overline{N}$ = 7.4, $\overline{N}_b$ = 3.7)

Discussion of analytic work.--The experience gained in this study simulating the line substitution error control scheme has clearly established the value of the technique for improving the reliability of compressed pictorial data transmitted over a binary symmetric channel. Line substitution error control, it may be recalled, operates in the following manner. It is known in advance that the sum of all the run length words on a picture line totals 450, corresponding to a total of 450 samples per line of uncompressed picture. Failure of a line to match this count leads to its rejection; the preceding picture line is then substituted in its place.

The line substitution technique has two important characteristics which led to its selection as the error control method for initial investigation. First of all, it requires no redundant bits or any other transmitted data modifications to achieve its error control capability. The inherent structure of the picture line data is utilized as an indicator of serious defect on a line while the high informational correlation between adjacent picture lines serves as a basis for providing an acceptable substitute for a defective line. A certain degree of error control is thereby achieved without the redundant transmitted bits associated with ordinary error-correcting codes. In addition, line substitution imposes little additional complexity upon the user; all that is required is sufficient memory to store a compressed picture line and a register to add up the run length words.

The efficacy of any data error control technique may be measured in terms of a "threshold" (maximum bit error probability) of channel quality beyond which data of acceptable quality cannot be extracted.

Our simulations and analytic approximations (which we shall discuss in detail later) indicate that ZOI and FOIOOT acting on the reconnaisance picture controlled by line substitution have as their threshold a bit error probability in the vicinity of 10^{-3}; the uncontrolled compressed picture is unacceptable when subjected to bit errors at this rate.

A question which logically arises is that of what further gains may be realized through the sacrifice of a modest reduction in data rate per unit of channel bandwidth, permitting the utilization of error-correcting coding have a fairly high ratio of information bits to redundant (parity check) bits. An error control approach representing the next stage of complexity above line substitution should satisfy the following desriability criteria:

1) It should impose a small redundancy penalty upon transmission. It would be reasonable to demand that no more than 1/4 of the transmitted bits are parity check bits.

2) It should be capable of utilization in a back-to-back combination with line substitution. The error-correcting coding will serve to restore many defective lines to acceptable condition. Decoding failures due to uncorrectable error patterns will usually be picked up by the application of a run length count and line substitution as required. Only a minority of decoding failures will lead to degraded picture lines.

3) It should concentrate its strength against run length word errors, which have been found to be more disruptive than errors in gray-level words. Maximum utilization of redundant bits is thereby achieved.

4) It should have a threshold error probability in the 10^{-2} region.

The (7, 4) Hamming coding scheme described below meets all these criteria. The description of the approach and of two others not having quite the same suitability in terms of these criteria are provided below. The alternate approaches are felt to possess considerable merit. The single parity check (SPC) code approach represents lower redundancy (and performance) than the (7, 4) Hamming code. The (15, 11) Hamming code might be used to provide nominally the same performance as the (7, 4) with a slight redundancy reduction bought by the use of more comlex coding.

The (7, 4) Hamming single-error-correcting code is a block code of length 7, in which the four information bits are protected by three parity check bits. Decoding, which may be accomplished quite simply, is illustrated for one variation of the code in Figure 31. Observe that if all three parity check equations are satisfied it is concluded that no bits are in error and the four information bits are read out. The other seven possible parity check outcomes each uniquely identify themselves with a single bit error pattern. Those four corresponding to information bit errors will necessitate changing of the appropriate information bit before readout.

(a) BLOCK OF 7 BITS

$$\underbrace{\boxed{X_1}\boxed{X_2}\boxed{X_3}\boxed{X_4}}_{\text{Information Bits}}\underbrace{\boxed{X_5}\boxed{X_6}\boxed{X_7}}_{\text{Redundant Bits}}$$

(b) PARITY CHECKS (ESTABLISHED ON TRANSMISSION)

i) $X_5 = X_2 \oplus X_3 \oplus X_4$

ii) $X_6 = X_1 \oplus X_3 \oplus X_4$

iii) $X_7 = X_1 \oplus X_2 \oplus X_4$

(c) PARITY CHECKS (PERFORMED UPON RECEPTION)

i) $Q_1 = X_1 \oplus X_3 \oplus X_5 \oplus X_7$

ii) $Q_2 = X_2 \oplus X_3 \oplus X_6 \oplus X_7$

iii) $Q_3 \quad X_4 \oplus X_5 \oplus X_6 \oplus X_7$

(d) SYNDROME = NUMBER TELLING ERROR LOCATION

$$S = 2^2 \cdot Q_3 + 2^1 \cdot Q_2 + 2^0 \cdot Q_1$$

For error in X_j, $S = j$.

For no errors, $S = 0$.

Figure 31 (7, 4) Single-Error-Correcting Code

With certainty any word containing a single error will be read out error-free. The response to a double error will always be the changing of another bit to create a block containing three errors but satisfying all three parity checks. For example, imagine that x_1 and x_5 are both in error. The parity check outcomes will be $Q_1 = 0$, $Q_2 = 0$, $Q_3 = 1$; thus $S = 4$ and the fourth bit will be changed. The decoding process is therefore seen as a "forced choice" procedure in which decoder failure is produced by multiple errors in a word.

The code is utilized for picture error control in the following manner, for use with compressed pictures employing a five bit run length word. Each significant sample word (6 bits of gray scale plus five bits of run length in ZOI, 6 bits of gray scale, one of offset, and five of run length in FOIOOT) has three parity check bits encoded with it. These three bits are the parity check bits upon the four most significant bits of the run length word. The least significant bit, corresponding to one horizontal resolution cell, is left unprotected, as are all six bits in the gray scale word.

There are two sorts of horizontal displacement errors which may be found in a decoded line. An error affecting an unprotected run word bit results in a single cell horizontal displacement on a line, an almost unnoticeable degradation. Multiple errors of this sort on a line might result in more severe degradation, depending upon the patterns of reinforcement and cancellation among these essentially random displacements. On the other hand, failure of a code block will throw one or more errors into the four protected bits of the run length word, generally creating a "large" horizontal displacement error.

Figure 32 indicates in diagrammatic form the tandem operation of a block error-correcting code and line substitution upon compressed picture data. It has been assumed that line synchronism is given by an end-of-line sequence which is essentially immune to failure for any values of bit error probability of interest(in any practical system, line synchronizing words will be far more immune to failure than data words). As shown, the data words on a line are decoded one at a time, and error correction is executed as required. As decoded, this line is fed into memory #1. The contents of memory #2 represent the most recent preceding "acceptable" line, the one which can be used as a substitute if necessary. An adder tallies the run length count from the beginning of the line. Subsequent to decoding the last significant sample word on the line, the accumulated count is compared to 450. If it does not differ from this correct number by more than some allowance value α, the line is plotted in the picture. Should it fall outside this allowable zone, the

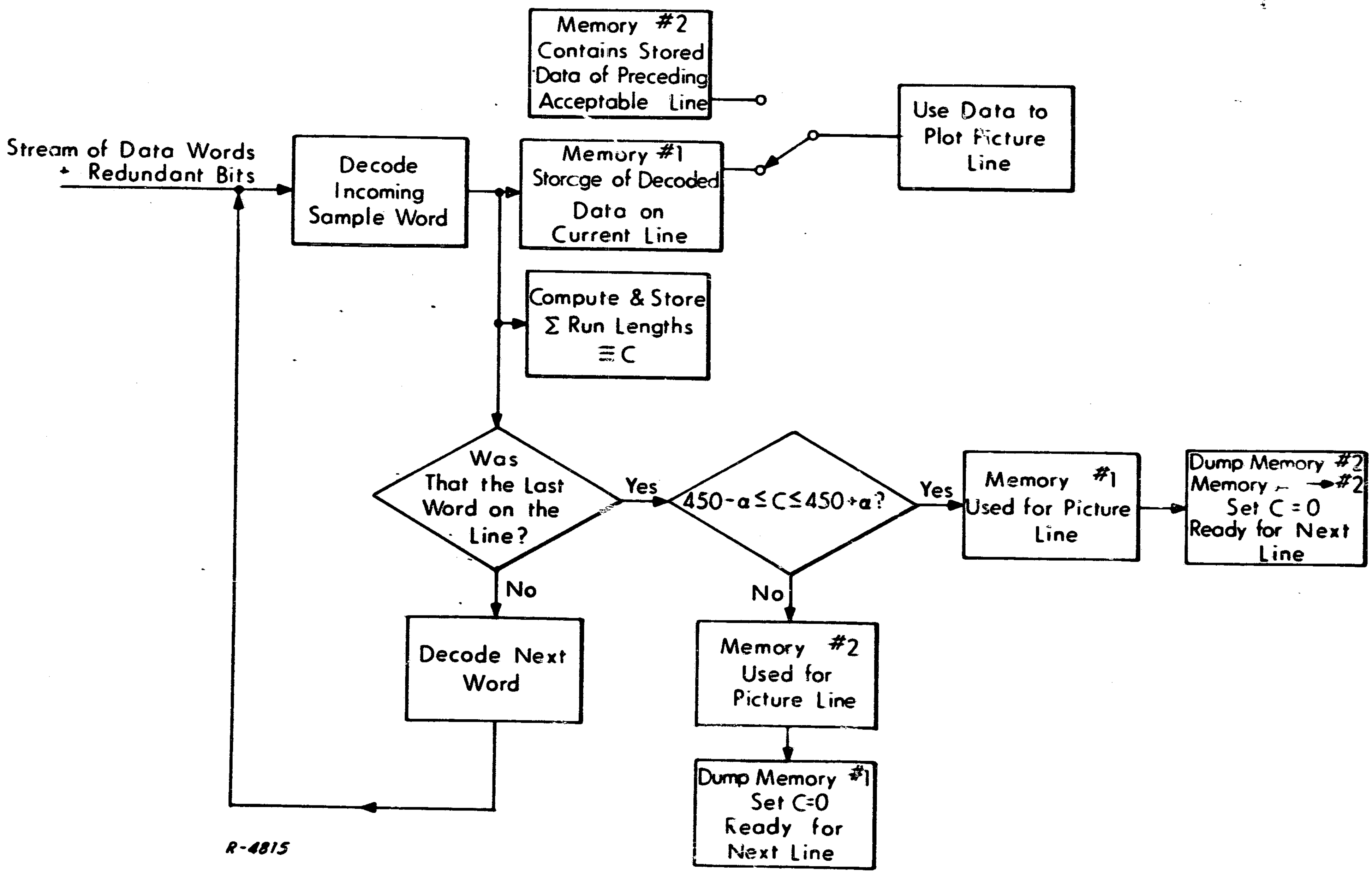

Figure 32 Diagrammatic Description of Method of Employing Error-Correcting Coding (One Code Block Per Significant Sample) In Tandem with Line Substitution Error Control on Compressed Video Pictures

preceding line (memory #2) is plotted as a substitute. (If there is no preceding line available , i. e., if failure occurs on the first line(s) of the picture, then plotting is suppressed until the first acceptable line is decoded.)

The notion of an allowance on the sum of the run length on a line was not used in the previous simulations employing ordinary line substitution. In these a line was rejected if it failed to have a total run word count of exactly 450 (allowance = 0). These simulations could have been performed with nonzero allowance; more will be said below about this possibility. The basic rationale built into the (7, 4) coding approach is that errors in the least significant bit are not of great importance. Three parity bits offer single error protection to the four most significant bits of the run length word in an optimal fashion: no fewer than three bits can do this job, and these three bits can protect a theoretical maximum of no more than four bits against single errors. The use of a zero allowance would be inconsistent with this underlying philosophy.

The (7, 4) coding scheme adds 3 bits to each 11-bit ZOI word or 12-bit FOIOOT word, resulting in effective data rate reductions of 21.4% and 20.0% respectively. The SPC coding approach requires only one redundant bit per sample word, producing data rate reductions of only 9.91% and 8.33% when used with ZOI and FOIOOT algorithms. SPC employs a single bit to provide even parity for the five bits of the run length word with which it is associated: Its binary value is chosen to produce an even number of 1's among the six bits involved. A check for even parity will detect the presence of any single bit failure in the word; double errors must go undetected. If one (and only one) word on a line has a single error, this error location may be noted as the line is being decoded and read into storage. If exactly one word on a line has been detected as in error, and if the final run length count differs from 450 by 1, 2, 4, 8, or 16 units, it is possible to go back into the stored line to the defective word and correct it. On the other hand, any of the following conditions indicate detection of errors which cannot be corrected, and therefore will lead to line substitution:

1) Two or more words detected to have parity check failure.

2) No words detected to have parity check failure, but discrepancy is present in end-of-line count. If the discrepancy is within the allowance value, the line will be accepted.

3) Only one word on a line detected to have parity check failure, but discrepancy not equal to 1, 2, 4, 8, or 16 is present in end-of-line count.

As will be seen, SPC is somewhat less effective than (7,4) coding. It is far simpler to encode and requires fewer redundant bits and the same storage capacity as the (7,4) coding. As a third alternative, the use of the (15,11) Hamming code will yield nominally the same performance as the (7,4) Hamming code with slightly greater complexity required for encoding and decoding. There are two ways in which (15,11) coding might be applied. The first (and less interesting) way is to encode each 11-bit ZOI word of 11 of the 12-bits of each FOIOOT word into a block. This would protect the gray scale words and increase the redundant bits by one per sample word. The second way is to let the run length words from two consecutive sample words plus a dummy bit form the eleven information bits of a block. Single error protection is extended to the ten bits of these two consecutive run length words; the redundancy is equal to two bits per word, i.e., a 15.5% data rate reduction with ZOI, and a 14.3% data rate reduction with FOIOOT.

Appendixes A through C provide analytic evaluations of these three error control schemes and the original line substitution scheme. The purpose of these analyses is to evaluate two quantities of merit for each scheme (as a function of bit error probability p): F_D, the fraction of lines in the final scanned picture which are "defective" (for one or more samples on the line, the horizontal displacement from the correct value exceeds the allowance value) and F_S, the fraction of lines which are "substitutes" (previous line replacing one detected as having error(s) which cannot be corrected). The analyses are done for allowance values α equal to 0,1, and 2.

There are certain general approximations which have been consistently employed throughout Appendixes A((7,4) coding and original line substitution schemes), B (SPC coding) and C((15,11) coding). It is first assumed that the number of significant samples on each line is $450/\overline{N}$, although in fact this quantity may possess wide statistical variation about its average value. "Small bit error probability" is also assumed. Important failures are often described with a single term as specified by the lowest order error pattern creating the failure; higher order error patterns are then neglected. These and other approximations are made consistent with the onjective of obtaining rough but meaningful estimates of performance for the schemes in question over regions of bit error probability for which the picture data is not completely "swamped".

Table 3 summarizes calculations performed utilizing the results of Appendixes A - C, for selected combinations of error control scheme, allowance value and bit error probability. For the one case (Ordinary Line Substitution, $\alpha = 0$, $p = 10^{-3}$) actually corresponding to a picture situation for which computer simulation was performed, there was found to be close agreement between the number of "substitute" lines in the simulated ZOI picture and the number indicated by the F_S value in Table 3.

Table III

ANALYTIC PERFORMANCE COMPARISON OF VARIOUS SCHEMES FOR PROTECTING 450 x 450 ELEMENT PICTURE TRANSMITTED OVER BINARY SYMMETRIC CHANNEL (ELEMENT COMPRESSION RATIO = 5.77:1), FOR VARIOUS VALUES OF BIT ERROR PROBABILITY

Scheme (coding, allowance value, bit error probability)	F_S	F_D
Ordinary Line Substitution, $\alpha = 0$, $p = 10^{-3}$	0.310	0.0075
Ordinary Line Substitution, $\alpha = 1$, $p = 10^{-3}$	0.255	0.0069
Ordinary Line Substitution, $\alpha = 2$, $p = 10^{-3}$	0.199	0.0051
(7,4) Code + Line Substitution, $\alpha = 1$, $p=10^{-2}$	0.212	0.014
(7,4) Code + Line Substitution, $\alpha=2$, $p=10^{-2}$	0.112	0.0038
Single Parity Check Code and Line Substitution $\alpha = 1$, $p = 2 \cdot 10^{-3}$	0.241	0.00001
(15,11) Code* + Line Substitution $\alpha = 1$, $p = 10^{-2}$	0.254	0.048
(15,11) Code* + Line Substitution $\alpha = 2$, $p = 10^{-2}$	0.242	0.040

F_S ≡ Fraction of lines which are substitutes

F_D ≡ Fraction of lines which are defective

* Two 5-bit run length words plus one dummy bit coded to form a block.

Several general observations may be made regarding the results in Table 3. It is quite clear that for a given coding scheme and bit error probability F_S and F_D tend to decrease as the allowance value is made larger. This merely reflects the truism that a loosened criterion of acceptability will permit a greater fraction of the data lines to be classified as acceptable. An interesting and significant question, which can hopefully be answered by detailed subjective evaluations under some future effort, is whether there is perhaps some "optimum" way to set the allowance criterion to provide maximum reconstructed picture quality in a given noise environment. Too large an allowance value will prevent the filtering out of many degraded lines, while too small a value will result in the use of substitute lines in place of lines with very minor errors.

Comparisons of Ordinary Line Substitution, (7, 4) Coding, SPC Coding and (15, 11) Coding for $\alpha = 1$ may be made from Table 3. (7, 4) Coding has an indicated ability to provide picture quality at $p = 10^{-2}$ roughly equivalent to that of Ordinary Line Substitution at $p = 10^{-3}$, representing an increase of the error rate threshold by a full order of magnitude. The SPC coding technique provides a limited gain over simple line substitution, matching it in performance at $p = 2.10^{-3}$. The (15, 11) coding turns out to offer a performance advantage which is very nearly the equal of that provided by (7, 4) coding.

Discussion of picture simulations.--Figure 26 simulates the result of transmitting the PCM uncompressed data of the detailed reconnaisance photo over a binary link randomly introducing bit error with probability 10^{-3}. The degradation with respect to the original (Figure 15) is seen to be negligible. This stands in sharp contrast to the serious degradation produced by this same error probability acting on a ZOI compressed picture as documented in Ref. 1. Figure 27 is the ZOI compressed "noisy" picture (repeated here in higher quality achieved with the JPL plotter as are the other pictures in Ref. 1) at 10^{-3} error probability. Figure 28 shows the substantial improvement obtained by the use of line substitution for error control with an allowance value of $\alpha = 0$. Approximately one-third of the lines in the picture have been filled in by substitution; one can locate parts of the picture where smooth contours have been rendered as "steps" due to consecutive line failures necessitating consecutive repetitions of the same picture line. Figures 29 and 30 represent a pair of FOIOOT compressed noise-perturbed pictures without and with line substitution ($\alpha = 0$) for error control. The above remarks regarding Figures 27 and 28 represent an equally valid description of these pictures.

A simulated picture showing the effects of a 10^{-2} bit error probability upon a FOIOOT compressed picture protected by the (7, 4) coding line substitution scheme was planned for inclusion in this report. This simulation has unfortunately not yet been completed, due to unanticipated programming difficulties. It is believed that this reconstructed picture, for an allowance value $\alpha = 2$, will show quality visibly superior to that of Figures 28 and 30.

REFERENCES

1. Interim Scientific Report, "Development of Advanced Digital Techniques for Data Acquisition Processing and Communication", 1 November 1967, by ADCOM, Inc., for NASA Electronics Research Center, Contract NAS12-554 (DO-C9).

PRECEDING PAGE BLANK NOT FILMED.

Appendix A

ANALYSIS OF (7, 4) CODING AND ORIGINAL LINE SUBSTITUTION APPROACH

The assumed characteristics of the data are as follows. Each line consists of $\bar{S} \cong 450/\bar{N}$ significant samples after compression. These samples contain 6 (or in the case of the FOIOOT algorithm, 7) bits each for intensity and 5 bits for run length.

For convenience the bits in the run word, which will receive protection from error-control coding, are referred to in order of decreasing significance as the 2^4-bit, the 2^3-bit, ... the 2^0-bit. The (7, 4) single-error-correcting code block associated with each sample ignores the 2^0-bit. A single error in any of the four most significant bits or one of the three parity check bits will always be corrected.

The assumed channel disturbance is one of independent equiprobable occurrence of bit errors with probability p. The dominant cause of decoding failure will be two bit errors in a block. (It may be shown that when this occurs, any of the four decoded run word bits are in error with probability 3/7). The probability of occurrence of a double error (the most likely uncorrectable pattern) in a word block is:

$$P(2/7) = \binom{7}{2} p^2(1-p)^5 = 21p^2(1-p)^5 \qquad \text{(A-1)}$$

The response of the decoder to the double error will be to change one bit. This will, for the Hamming code, surely create another codeword satisfying all parity checks, but differing from the transmitted word by virtue of three bit changes.

Note that the decoder action in this situation consists of the 'addition' (modulo 2, bit-by-bit) of an error pattern which must be a codeword of weight 3 to the transmitted word. Such a codeword in a parity check code, as may beshown by more rigorous arguments, must have at least one nonzero information bit. Hence, it may be concluded that a double bit error leads to failure of one or more of the run length bits read out after decoding. Thus P_w, the probability of a decoded word error, is well approximated by:

$$P_w \approx P(2/7) = 21p^2 (1-p)^5 \qquad p \ll 1 \qquad \text{(A-2)}$$

On the basis of $\overline{S}$ run length words on a line, the probability of one or more failures in the 2^1 through 2^4 bits of run length words on a line is:

$$P_L = 1 - (1 - P_w)^{\overline{S}} \qquad \text{(A-3)}$$

The very great majority of these errors will be detected because either: a) there is only one such error on the line, and the end-of-line count will be indicative of the error magnitude or b) there are two or more errors, but they do not cancel.

A second occurrence leading to failure to have a proper end-of-line count is errors in the $\overline{S}$ unprotected least significant bits of run length words. We evaluate this phenomenon below. Note that we are ignoring a factor of mild importance in order to keep the analysis tractable. This is the interaction of these two types of errors. They will sometimes tend to cancel and sometimes tend to add. The effect of this interaction in influencing the occurrence of lines failing the count and the occurrence of 'bad' lines with severe count errors in mid-line which go undetected because of later complementary errors has therefore been ignored in our analysis.

When the allowance is zero, i.e., when a line must have a count of exactly 450 to be accepted, an unacceptable line may sneak through due to the canceling effects of word errors. We consider the dominant event of this type to be due to two word errors. The numerical error in a run length word is due to one, two, or occasionally three individual bit errors. Error components of magnitude ±16, ±8, ±4, or ±2 horizontal cells will add up to give an error which may be canceled by another of equal magnitude but of opposite sign. The probability of occurrence of such errors depends upon the a priori probabilities of occurrence of 0's and 1's in the different positions of run length words, which in turn depends upon the compression process (for example, when the average compression ratio is about 5:1, the 2^4 -bit will almost always be a '0').

To gain a rough estimate of a quantity which is so impossible to calculate, it must be assumed that the four bits assume binary values equiprobably, and that a decoding failure throws an error into one of them. Then 1/4 of the time the errors in two words will be in corresponding bits and one half of that time they will be of opposite type, i.e., a 0-1 transposition in one canceling a 1-0 transpostition in the other. The probability of a line being made undetectably 'bad' by word errors is thus:

$$P_u^{(0)} = \frac{1}{8}\binom{\overline{S}}{2} P_w^2 (1 - P_w)^{\overline{S}-2} = \left[\frac{\overline{S}(\overline{S}-1)}{16}\right] \cdot P_w^{\,2} (1 - P_w)^{\overline{S}-2} \qquad \text{(A-4)}$$

The same description of production of defective pictu. lines by this phenomenon will hold when an allowance of ±1 on the run count constitutes the criterion of acceptability. (A line must have a final count of 449 -451 to be accepted. A line which has any sample location in error by two or more horizontal cells, but passes the end-of-line count test is an undetectably bad line.)

$$P_u^{(1)} = P_u^{(0)} = \left[\frac{\bar{S}(\bar{S}-1)}{16}\right] \cdot P_w^{\ 2}(1-P_w)^{\bar{S}-2} \qquad \text{(A-5)}$$

The evaluation of this sort of occurrence when the allowance is ±2 cells is slightly more complicated. We again simplify by considering two words in error, each having only one of the four most significant run length word bits in error. In addition to the errors that were troublesome with the tighter allowance, the pattern of an error in the 2^2 digit of one word and an opposite polarity error in the 2^1 digit of the other becomes dangerous. Thus it is easily reasoned that:

$$P_u^{(2)} = (5/32)\binom{\bar{S}}{2} P_w^{\ 2}\ (1-P_w)^{S-2} = \left[\frac{5\ \bar{S}(\bar{S}-1)}{64}\right] P_w^{\ 2}(1-P_w)^{\bar{S}-2} \qquad \text{(A-6)}$$

The other contribution to undetectably bad lines is multiple errors in the unprotected least significant bit. The symbol B(j) will denote the probability that exactly j out of the $\bar{S}$ unprotected bits are in error:

$$B(j) = \binom{\bar{S}}{j} p^j\ (1-p)^{\bar{S}-j} \qquad \text{(A-7)}$$

If the allowance is zero, any line having an error in one or more of the unprotected bits is an unacceptable line. It will not be detected on a count basis if the number of such errors is even and is composed of an equal number of 0-1 transpositions and 1-0 transpositions. There are 2^j possible patterns of j transpositions; the undetectable ones are those $\binom{j}{j/2}$ having j/2 of the 0-1 type. Under the assumption of equiprobability of the unprotected bits, all j transposition patterns occur with equal probability. The the probability of a line being made undetectably bad by errors of this sort is:

$$P_x^{(0)} = \frac{1}{2} \cdot B(2) + \frac{3}{8} \cdot B(4) + \frac{5}{16} B(6) + \ldots \qquad \text{(A-8)}$$

If the allowance is extended to ±1 horizontal cell, it becomes necessary to go to an exhaustive study of transposition patterns to perform our evaluation. The symbols a and b are used below to denote the 0-1 type and 1-0 type transpositions. Those patterns which contributed to producing undetected bad lines are indicated by underlining. They:

i) have at some point in their first m places, $m = 1, 2, \ldots j-1$, a run-out (excess of a's over b's or excess of b's over a's) exceeding the allowance, and

ii) have a run-out within the allowance when $m = j$, i.e., at the end of the pattern.

The patterns are as follows:

3 Transpositions:	aaa;	$\underline{\text{aab}}$;	aba;	abb
	baa;	bab;	$\underline{\text{bba}}$;	bbb

4 Transpositions:	aaaa;	aaab;	aaba;	$\underline{\text{aabb}}$;
	abaa;	abab;	abba;	abbb;
	baaa;	baab;	baba;	babb;
	$\underline{\text{bbaa}}$;	bbab;	bbba;	bbbb

5 Transpositions:	aaaaa;	aaaab;	aaaba;	$\underline{\text{aaabb}}$;
	aabaa;	$\underline{\text{aabab}}$;	$\underline{\text{aabba}}$;	$\underline{\text{aabbb}}$;
	abaaa;	$\underline{\text{abaab}}$;	ababa;	ababb;
	abbaa;	abbab;	$\underline{\text{abbba}}$;	abbbb;
	baaaa;	$\underline{\text{baaab}}$;	baaba;	baabb;
	babaa;	babab;	$\underline{\text{babba}}$;	babbb;
	$\underline{\text{bbaaa}}$;	$\underline{\text{bbaab}}$;	$\underline{\text{bbaba}}$;	bbabb;
	$\underline{\text{bbbaa}}$;	bbbab;	bbbba;	bbbbb

On the basis of the above, it is clear that:

$$P_x^{(1)} = \frac{1}{4} \cdot B(3) + \frac{1}{8} \cdot B(4) + \frac{3}{8} \cdot B(5) + \ldots \qquad \text{(A-9)}$$

The same procedure may be reapplied using a ±2 cell allowance. Transposition patterns are written out again, with underlining to denote those contributing to $P_x^{(2)}$.

4 Transpositions:	aaaa;	$\underline{\text{aaab}}$;	aaba;	aabb;
	abaa;	abab;	abba;	abbb;
	baaa;	baab;	baba;	babb;
	bbaa;	bbab;	$\underline{\text{bbba}}$;	bbbb

5 Transpositions: aaaaa; aaaab; aaaba; aaabb;
aabaa; aabab; aabba; aabbb;
abaaa; abaab; ababa; ababb;
abbaa; abbab; abbba; abbbb;
baaaa; baaab; baaba; baabb;
babaa; babab; babba; babbb;
bbaaa; bbaab; bbaba; bbabb;
bbbaa; bbbab; bbbba; bbbbb

Thus:

$$P_x^{(2)} = \frac{1}{8} \cdot B(4) + \frac{1}{16} \cdot B(5) + \ldots \qquad \text{(A-10)}$$

Keep in mind that there are only two decisions which may be made upon a line: 'Reject' (and substitute preceding line) or 'Accept'. We have now derived the components contributing to an erroneous decision to accept. Next the probability of a line being rejected must be derived. A rejection of a line is never erroneous, since a line will be rejected only if there are real errors in it. Rejected lines will arise from the two mechanisms of decoding failures and accumulated errors in unprotected bits.

Those word errors which do not cancel out will contribute to rejected lines. The symbol $P_L^{(i)}$ denotes the probability of a line having errors in protected bits which are unacceptable within the allowance criterion.

$$P_L^{(i)} = \begin{cases} P_L, & i = 0 \\ P_L, & i = 1 \\ \frac{3}{4} \cdot P_L, & i = 2 \end{cases} \qquad \text{(A-11)}$$

The assumption used in Eq. (A-11) above is that $P_L^{(i)}$ is strongly dependent upon the single word error patterns. For $i = 0$ and $i = 1$, these always produce unacceptable lines. For $i = 2$, on the assumption of 1 bit in error, the 1/4 of the time that it is the 2^1 bit the line need not be rejected.

Using Eq. (A-3) through (A-6) and Eq. (A-11) above:

$$P_R^{(i)} = P_L^{(i)} - P_u^{(i)} \qquad i = 0, 1, 2 \qquad \text{(A-12)}$$

where the integer i denotes the allowance criterion, and $P_R^{(i)}$ is the probability of a line being rejected due to errors in the protected bits.

The occurrence of line rejections due to errors in unprotected bits is easily evaluated. Consider first the zero allowance case. A rejection decision must always arise from any odd number of errors in these bits. One will also arise from any even number of transpositions when 0-1 types and 1-0 types are not present in equal quantity, e.g., all but $\binom{4}{2}$ of the 2^4 4-transposition patterns.

$$P_s^{(0)} = B(1) + \frac{1}{2} B(2) + B(3) + \frac{5}{8} B(4) + B(5) + \ldots \qquad \text{(A-13)}$$

If the allowance is ±1 horizontal cell, then rejections will arise from transpostition patterns having an excess of two or more of one type of transposition over the other. This includes 2 of the 4 2-transposition patterns, 2 of the 8 3-transposition patterns; $2\cdot\binom{4}{0} + 2\binom{4}{1}$ of the 16 4-transposition patterns, and $2\cdot\binom{5}{0} + 2\binom{5}{1}$ of the 32 5- transposition patterns.

$$P_s^{(1)} = \frac{1}{2} B(2) + \frac{1}{4} B(3) + \frac{5}{8} B(4) + \frac{3}{8} B(5) + \ldots \qquad \text{(A-14)}$$

For an allowance of ±2 cells:

$$P_s^{(2)} = \frac{1}{4} B(3) + \frac{1}{8}\cdot B(4) + \frac{3}{8}\cdot B(5) \qquad \text{(A-15)}$$

The proper assembly of all the above results can yield two important parameters in the description of picture degradation due to bit errors: F_s, the fraction of lines in the picture which are substitutes, the preceding line replacing a line detected to have errors, and F_D, the fraction of lines presented in the picture which are defective in terms of the allowance criterion.

A given line will be substituted for by the preceding line if it is either rejected on account of protected bit errors with probability $P_R^{(i)}$ or if it is rejected due to unprotected bit errors with probability $P_s^{(i)}$. If these probabilities are assumed to represent mutually exclusive and independent events:

$$F_s = 1 - (1 - P_R^{(i)}) \cdot (1 - P_s^{(i)}) \qquad i = 0, 1, 2 \qquad \text{(A-16)}$$

The probability that a line will be undetectably defective is similarly expressible as:

$$P_D = 1 - (1 - P_u^{(i)}) \cdot (1 - P_x^{(i)}) \qquad i = 0, 1, 2 \qquad \text{(A-17)}$$

But the fraction of defective lines in the picture will be somewhat larger than P_D. Observe that the line immediately following a defective line will require substitution with probability F_s. Defective lines may come in sequences. An isolated defective line occurs with probability $P_D \cdot (1-F_s)$, two consecutive defective lines with probability $P_D \cdot F_s \cdot (1-F_s)$. . . m consecutive defective lines with probability $P_D \cdot F_s^{m-1} \cdot (1-F_s)$. Thus:

$$F_D = P_D \cdot (1-F_s) + 2P_D \cdot F_s(1-F_s) + 3P_D \cdot F_s^2(1-F_s) + mP_D \cdot F_s^{m-1} \cdot (1-F_s) + \ldots$$

$$= \frac{P_D}{1-F_s} \qquad \text{(A-18)}$$

Appropriate use of Eqs. (A-1) through (A-15) in Eqs. (A-16) and (A-18) will result in calculations of the values of F_s and F_D for values of p and allowance criterion of interest.

The corresponding analysis of noise effects when the error control for the compressed data consists solely of the line substitution scheme may now be worked out. $\overline{S}$ 5-bit run length words are assumed to occupy each line. C(j) is defined to be the probability of exactly j errors in the $5\overline{S}$ bits of the run length words.

$$C(j) = \binom{5\overline{S}}{j} p^j (1-p)^{5\overline{S}-j} \qquad \text{(A-19)}$$

In discussing the production of undetectably bad lines, we shall be concerned with patterns consisting of a very few bit transpositions on a line. We shall assume that such errors are so distributed that no single run word has two errors; this is by far the most likely occurrence. It is necessary to introduce a bit of notation at this point. One of the $\overline{S}$ possible (all assumed equiprobable) patterns of double bit errors might be $[+2^2, -2^0]$. This would indicated that the first error was a 0-1 transposition in a 2^2-bit of some word, and the second was a 1-0 transposition in the 2^0-bit of a later word on the line.

If the allowance is zero, the only two-error patterns that will not be detected will be of the form $[+2^{2}, -2^{j}]$ or $[-2^{j}, +2^{j}]$. This is the fraction 1/10 of the total.*

The contribution of 3-error patterns is considerably smaller, and may be ignored without serious error. This is true because a smaller fraction of 3-error patterns are dangerous, and also because C(3) is considerably smaller than C(2). For the highest error probability of interest, $p = 10^{-3}$, $C(2) \div C(3) \approx 6.0$.

$$P_y^{(0)} = \frac{1}{10} \cdot C(2) \qquad \text{(A-20)}$$

When the allowance is ±1, the following double error patterns generate undetectably bad lines:

$$[\pm 2^1, \mp 2^1];\ [\pm 2^1, \mp 2^0];\ [\pm 2^2, \mp 2^2];\ [\pm 2^3, \mp 2^3];\ [\pm 2^4, \mp 2^4]$$

Hence:

$$P_y^{(1)} = \frac{1}{10} \cdot C(2) \qquad \text{(A-21)}$$

The following double error patterns are troublesome when the allowance is ±2:

$$[\pm 2^2, \mp 2^1];\ [\pm 2^2, \mp 2^2];\ [\pm 2^3, \mp 2^3];\ [\pm 2^4, \mp 2^4]$$

$$P_y^{(2)} = \frac{2}{25} \cdot C(2) \qquad \text{(A-22)}$$

A given line will be put into the 'substitute' category only if the final count falls outside the allowance. We shall consider only the contributions of single and double errors to the presence of rejected lines.

*There are 100 possible combinations of the form $[+2^{i}, -2^{j}]$ or $[-2^{i}, +2^{j}]$ over all, $i, j = 0, 1, 2, 3, 4$. These represent the totality of all two-error patterns.

Under an allowance of zero, the probability that a line will be marked for substitution is:

$$
\begin{aligned}
P_T^{(0)} &= 1 - C(0) - P_y^{(0)} \\
&= 1 - C(0) - \frac{1}{10} \cdot C(2) \\
&\approx C(1) + \frac{9}{10} \cdot C(2)
\end{aligned}
\tag{A-23}
$$

Equation (A-23) above notes that any error at all makes a line unacceptable. Those not slipping through undetected must therefore lead to line repetition.

If the allowance is ±1, then a single error in any bit other than the 2^0 bit will lead to line repetition. Out of the 100 double-error patterns, it has already been shown that 10 produce undetectably bad lines. In addition, the following produce line defects which are 'allowable', and will not lead to rejection.

$$[\pm 2^0, \mp 2^0]; \; [\pm 2^0, \mp 2^1]$$

Consequently:

$$P_T^{(1)} = \frac{4}{5} \cdot C(1) + \frac{43}{50} \cdot C(2) \tag{A-24}$$

Under an allowance rule of ±2, only single errors in one of the three highest order bits of a word will lead to a line rejection. The 'allowable' double-error patterns are:

$$[\pm 2^0, \mp 2^0]; \; [\pm 2^0, \mp 2^1]; \; [\pm 2^1, \mp 2^0]; \; [\pm 2^1, \mp 2^1]; [\pm 2^1, \mp 2^2]$$

$$P_T^{(2)} = \frac{3}{5} \cdot C(1) + \frac{4}{5} \cdot C(2) \tag{A-25}$$

Utilizing the results stated in Eqs. (A-19) -(A-25), evaluations of the fraction of picture lines which are substitutes and the fraction which are defective may be carried out:

$$F_S = P_T^{(i)} \qquad i = 0, 1, 2 \tag{A-26}$$

$$F_D = \frac{P_y^{(i)}}{1 - P_T^{(i)}} \qquad i = 0, 1, 2 \tag{A-27}$$

PRECEDING PAGE BLANK NOT FILMED.

Appendix B

ANALYSIS OF SINGLE PARITY CHECK CODING

The single parity check coding technique employs a single redundant bit for each run length word. This bit serves to check even parity, i.e., its binary value is chosen to produce an even number of 1's among the six bits involved. It is possible to detect the presence of any single bit failure in a word by parity failure; double errors must go undetected. If one (and only one) word on a line has a single error, this error location may be noted as the entire line is fed into storage. The error in the run length count, 1, 2, 4, 8 or 16 units, will indicate the magnitude of this error. It is then possible to go back and correct it. On the other hand, any of the following conditions indicate detection of errors which cannot be corrected, and therefore will lead to line substitution:

(a) Two or more words detected to have parity check failure;

(b) Only one word on line detected to have parity check failure, but discrepancy is not equal to 1, 2, 4, 8, or 16 is present in end-of-line count.

(c) No words detected to have parity check failure, but discrepancy is present in end-of-line count. If the discrepancy is within the allowance, the line will not be rejected.

Exactly $\bar{S}$ 6-bit protected run length words per picture line are assumed. The probability that exactly j bits out of the total of $6\bar{S}$ are in error may be denoted by D(j)

$$D(j) = \binom{6\bar{S}}{j} p^j (1-p)^{6\bar{S}-j} \qquad \text{(B-1)}$$

Almost all the time that there are two or more bit errors on a line, the result will be a substitution decision (only a small fraction of triple and higher order errors will slip through undetected).

$$P_L = D(2) + D(3) + \ldots \qquad \text{(B-2)}$$

Equation (B-2) above has no significant variation as the allowance criterion is changed.

The occurrence of undetectably bad lines is an event dominated by 4-error patterns on a line putting two errors in each of two different words. If these undetected errors should cancel their presence would go undetected. The probability of a 6-bit word having an undetected error is

$$P_w = \binom{6}{2} p^2 (1-p)^4 = 15\, p^2 (1-p)^4 \qquad \text{(B-3)}$$

Either one or two of the information-bearing bits in such a word will be in error. The numerical value of error associated with the word will cover the range of nonzero integers from -24 to +24, excluding the values ±11, ±13, ±19, ±21, ±22, ±23. The following reasonable assumption therefore suggests itself. Consider that the error covers a spread of 36 values equiprobably. Then the probability that the error value in the second word to fail exactly cancels the error value in the first is 1/36; the probability of cancellation within ±1 allowance is 1/12; and the probability of cancellation within ±2 allowance is 5/36. Consequently, one derives probabilities of undetected bad lines for the three allowance criteria

$$P_u^{(0)} = \left[\frac{\bar{S}(\bar{S}-1)}{72}\right] P_w^{\,2} (1-P_w)^{\bar{S}-2} \qquad \text{(B-4)}$$

$$P_u^{(1)} = \left[\frac{\bar{S}(\bar{S}-1)}{24}\right] P_w^{\,2} (1-P_w)^{\bar{S}-2} \qquad \text{(B-5)}$$

$$P_u^{(2)} = \left[\frac{5\bar{S}(\bar{S}-1)}{72}\right] P_w^{\,2} (1-P_w)^{\bar{S}-2)} \qquad \text{(B-6)}$$

Thus, the fraction of lines in a picture which are substitutes is

$$F_s = P_L \qquad \text{(B-7)}$$

And the fraction which is defective is

$$F_D = \frac{P_u^{(i)}}{1 - P_L} \qquad i=0,1,2 \qquad \text{(B-8)}$$

APPENDIX C

ANALYSIS OF (15, 11) SINGLE-ERROR-CORRECTING CODING

Consider first the case in which the (15, 11) single-error-correcting block code uses its four check bits to effect full control of single errors in any of eleven bits in the coded word for a significant sample. Consequently all five run length word bits are protected and, in the case of the ZOI, all six gray-scale bits are protected as well; if the FOIOOT algorithm all but one of the seven bits for specifying gray-scale intensity and offset will be protected.

Our analysis, as in Appendixes A and B preceding, is directed toward analysis of the presence of substituted lines and defective lines in a displayed picture utilizing the combined error control of (15, 11) coding and line substitution. The improvement inherent in the reduction of errors in gray scale values of significant samples is acknowledge for this approach. But no specific comparisons are made. A picture line is assumed to consist of $\bar{S}$ (15-bit) words.

The probability of occurrence of the most likely source of word failure, a double error pattern, is

$$P(2/15) = \binom{15}{2} p^2 (1 - p)^{13} = 105 p^2 (1 - p)^{13} \qquad \text{(C-1)}$$

The decoding response to the double error will be to change one bit in the process of 'correcting' what it treats as a single error producing a block of 15 bits, three of which are in errors from which the eleven information bits are extracted. Five of these eleven are the run length word bits with which we concern ourselves. When such a decoding failure occurs it is likely that one of more of the run length word bits may suffer an error, though there may be word errors not affecting these bits at all. As a conservative approximation to actual occurrences, it will be assumed that a word failure results in a single bit failure

$$P_W \cong P(2/15) = 105 p^2 (1 - p)^{13} \qquad \text{(C-2)}$$

The probability of one or more such word failures on a line is

$$P_L = 1 - (1 - P_W)^{\bar{S}} \qquad \text{(C-3)}$$

Undetected bad lines may be evaluated by using the conservative assumption of one run length word bit in error in each word that fails. Thus

$$P_u^{(0)} = \frac{1}{10} \binom{\bar{S}}{2} P_w^2 (1 - P_w)^{\bar{S}-2} \approx \left[\frac{\bar{S}(\bar{S}-1)}{20}\right] P_w^2 (1-P_w)^{\bar{S}-2} \qquad \text{(C-4)}$$

If the allowance is ±1 horizontal cell, the undetected two-word error patterns are increased by the inclusion of opposite polarity errors in the 2^1 bit of one word and the 2^0 bit of the other. On the other hand, equal and opposite errors in the 2^0 bits must be excluded. There is a small net change in the number of dangerous error patterns

$$P_u^{(1)} = \frac{3}{25} \binom{\bar{S}}{2} P_w^2 (1 - P_w)^{\bar{S}-2} \approx \left[\frac{3S(S-1)}{50}\right] P_w^2 (1-P_w)^{\bar{S}-2} \qquad \text{(C-5)}$$

For a ±2 cell allowance, a count of dangerous two-word single error patterns results in

$$P_u^{(2)} = \frac{1}{10} \binom{\bar{S}}{2} P_w^2 (1 - P_w)^{\bar{S}-2} = \left[\frac{\bar{S}(\bar{S}-1)}{20}\right] P_w^2 (1-P_w)^{\bar{S}-2} \qquad \text{(C-6)}$$

Rejected lines arise from among the fractional set P_L of lines in which the errors are detected and are not within the allowance criterion. The symbol $P_L^{(i)}$ denotes the probability of a decoded line having errors which are unacceptable within the allowance criterion.

$$P_L^{(i)} = \begin{cases} P_L & i = 0 \\ 4/5\ P_L & i = 1 \\ 3/5\ P_L & i = 2 \end{cases} \qquad \text{(C-7)}$$

where it has been assumed that $P_L^{(i)}$ is strongly dependent upon single word error patterns, and the single bit errors in run length words produced by them. For $i = 0$ these always produce unacceptable lines; for $i = 1$, an error in the 2^0 bit is allowable; for $i = 2$, an error in the 2^0 bit or in the 2^1 bit is allowable.

The fraction of lines in the picture which are substitutes may be stated as

$$F_s = P_L^{(i)} - P_u^{(i)} \qquad i = 0, 1, 2 \qquad \text{(C-8)}$$

The fraction of defective lines in the picture may be stated as

$$F_D = \frac{P_u^{(i)}}{1 - F_s} \qquad i = 0, 1, 2 \tag{C-9}$$

The above analysis may be extended to apply to the case in which two consecutive 5-bit run length words plus a dummy bit are encoded in a block. There are now an assumed $\bar{S}/2$ code blocks on a line. The probability of one or more of these blocks failing is simply:

$$\hat{P}_L = 1 - (1 - P_w)^{\bar{S}/2} \tag{C-10}$$

where P_w is given by Eq. (C-2) above.

We assume that the contribution to rejected and defective lines comes from single block failures. A single block failure is considered to throw a single bit error into each of the two adjacent run length words coded together into a block. In the case $i = 0$, the cancellation of equal and opposite errors will lead to an undetected error situation:

$$\hat{P}_u^{(0)} = \frac{1}{10} \cdot \hat{P}_L \tag{C-11}$$

Similarly:

$$\hat{P}_u^{(1)} = \frac{3}{25} \cdot \hat{P}_L \tag{C-12}$$

$$\hat{P}_u^{(2)} = \frac{1}{10} \cdot \hat{P}_L \tag{C-13}$$

Straight forward procedures lead to evaluation of F_S. For $i = 0$

$$\hat{F}_S = \frac{9}{10} \hat{P}_L \tag{C-14}$$

Equation (C-14) above states that except when equal and opposite errors cancel, a decoding failure leads to a line substitution. Similarly

$$\hat{F}_S = \frac{21}{25} \cdot \hat{P}_L \qquad i = 1 \tag{C-15}$$

$$\hat{F}_S = \frac{4}{5} \cdot \hat{P}_L \qquad i = 2 \tag{C-16}$$

The fraction of detective lines is:

$$\hat{F}_D = \frac{\hat{P}_u^{(i)}}{1 - \bar{F}_S} \qquad i = 0, 1, 2 \qquad \text{(C-17)}$$

Appendix D

NEW TECHNOLOGY

After a diligent review of the work performed under this contract, no new innovation, discovery, improvement or invention was made.

PRECEDING PAGE BLANK NOT FILMED

ACKNOWLEDGMENTS

The authors would like to express their appreciation for the assistance of the Jet Propulsion Laboratory in making available to us Surveyor I photographs and for reproducing the compressed data photographs used in this report. In particular, we gratefully acknowledge the assistance of Fred Billingsley, Roger Brandt, Elbert Johnson and Jack Lindsley. In addition, we appreciate the assistance of Dr. Jaffe of the Surveyor Project Office for permitting us to incorporate Surveyor data in this report.